



HYDROGEOLOGICAL ASSESSMENT
OF SPRINGS AND GROUNDWATER IN
CARRIZAL, COSTA RICA

LUND UNIVERSITY

Markus Beckman

Jacob Sannum

Division of Engineering Geology
Faculty of Engineering
Lund University

MSc Thesis, 30 ECTS

ISRN LUTVDG/(TVTG-5169)/1-51/(2020)



Thesis work for Master of Science 30 ECTS
Engineering Geology, LTH, Lund University

HYDROGEOLOGICAL ASSESSMENT OF SPRINGS AND GROUNDWATER IN CARRIZAL, COSTA RICA

Markus Beckman
Jacob Sannum

Division of Engineering Geology
Faculty of Engineering
Lund University

Lund 2020

ISBN LUTVDG/(TVTG-5169)/1-51/(2020)

Supervisor Master Thesis

Alfredo Mendoza, Engineering Geology

Assistant Supervisors

Oscar Vega Leonardo, Universidad Técnica Nacional (UTN) de Alajuela
Yemerith Alpizar Segura, Universidad Técnica Nacional (UTN) de Alajuela

Examiner

Jan-Erik Rosberg, Engineering Geology

This study was performed within the framework of The Minor Field Studies (MFS) Scholarship Programme, which is funded by the Swedish International Development Cooperation Agency, Sida. The responsibility for the accuracy of the information presented in this MSc thesis rests entirely with the authors.

Acknowledgements

This master thesis is the final examination for Jacob and Markus in the programme Environmental Engineering at Lund University. We are thankful for the opportunity to conduct it as a “Minor Field Study” and contribute to the Swedish international development work as representatives of Sida. Profound gratitude towards our supervisor Alfredo Mendoza who has assisted us all the way from contacting the university in Costa Rica to supporting us in finalizing the writing of this thesis. We also give much appreciation to Universidad Técnica Nacional, our local supervisors Yemerith Alpizar and Oscar Vega, for the cooperation, positive communication, and hospitality both in Costa Rica and digitally. Finally, we extend a huge thanks to the people in Carrizal; Guiselle Mejias-Alvarez, Ana-Patricia Barrantes and Antonio Mejias Castro, without them the fieldwork would not have been possible, muchas gracias.

Abstract

The main purpose of this thesis is to increase the understanding of how hydrogeological conditions are affecting the local water resources in Carrizal on the Barva Volcano, Costa Rica. Hydrogeological investigations of spring characteristics, soil infiltration rates and water flow in springs and rivers were conducted at the study area in Costa Rica as part of a Minor Field Study (MFS). A statistical analysis comparing spring flow rates and precipitation, based on data collected by Costa Rican organisations during several years, led to the conclusion of a potential water age of 0-24 months in aquifers discharging in the assessed springs. A recent decrease of flowrate in the local springs on the volcano can therefore be explained by less precipitation than the average in the years 2018 and 2019.

Spatial and temporal variabilities in spring flow, change in groundwater storage (ΔS) and precipitation patterns were analysed to determine groundwater flow systems communicating with springs in the study area. However, specific groundwater recharge areas were hard to delimit since possibly multiple flow systems were found to be communicating with the same spring. Overall high values of ΔS were calculated from the water balances but more research is needed to see if this contributes to Mountain Block Recharge (MBR) or discharges in unstudied areas further down on the volcano.

Keywords: Hydrogeology, volcanic aquifer, Water balance analysis, MBR, Costa Rica, double ring infiltrometer, spring characteristics, minor field study.

Table of contents

1.	Introduction	1
1.1	Background	1
1.2	Purpose and objectives	1
1.3	Methodology.....	2
1.3.1	Desktop studies.....	2
1.3.2	Fieldwork.....	2
1.3.3	Statistical data analysis	2
1.3.4	Water balance analysis	2
2.	Theoretical background	3
2.1	Hydrological cycle	3
2.1.1	Groundwater occurrence.....	4
2.1.2	Groundwater recharge in mountainous areas.....	5
2.1.3	Springs.....	5
2.2	Volcanic geology	6
3.	Description of study area.....	7
3.1	Carrizal	7
3.2	Climate	8
3.3	Geological setting on the Barva volcano.....	9
3.4	Previous hydrogeological studies near Carrizal	11
4.	Methods.....	12
4.1	Site investigations and measurements.....	12
4.1.1	Ocular assessment of springs.....	12
4.1.2	Infiltration	12
4.1.3	Flow measurements in rivers and springs	14
4.2	Data analyses	15
4.2.1	Statistical data analysis	15
4.2.2	Water balance analysis	15
5.	Results and discussion	18
5.1	Fieldwork.....	18
5.1.1	Springs.....	19
5.1.2	Infiltration	21
5.1.3	Rivers.....	26
5.1.4	Summary of fieldwork results	28
5.2	Statistical data analysis	29
5.2.1	Monthly comparison.....	29

5.2.2 Annual comparison	31
5.3 Water balance analysis	33
5.4 Conceptual model of groundwater flow systems	37
6. Conclusions	39
6.1 Recommendations	40
References	41
Appendix	43
A: Available data	43
B: Springs.....	47
C: Data analyses	48
D: Well Reports	50

1. Introduction

1.1 Background

There are growing concerns for the water resources used by local water administrators in Carrizal, operating on the southwest slope of the Barva volcano in Costa Rica. Potable water produced in the area is extracted from springs which have shown a decrease in flow over the last two years. The water organisation is worried that an increased amount of land exploitation in the area could jeopardise the water resources which would counteract the UN Sustainable Development Goal (SDG) number 6. SDG number 6 acts to ensure availability and sustainable management of water and sanitation for all. To validate the worries of the water organisation an assessment of the groundwater and springs in the area is needed.

Mechanism of groundwater recharge in volcanic areas with steep slopes are poorly understood and there are yet no consensus of the best way of assessing it. Previous tested methods have been related to the specific type of geological setting and previous knowledge of the area (Markovich et al., 2019). For the area around Carrizal, a water balance analysis supported by field measurements is recommended by Schosinsky (2005) to increase the knowledge of where groundwater recharge might occur and what type of groundwater flow system the springs are connected to.

1.2 Purpose and objectives

The main purpose of this thesis is to increase the understanding of how hydrogeological conditions are affecting the local water resources in Carrizal, Costa Rica. A water balance analysis supported by site investigations is proposed to make a hydrogeological assessment of springs and groundwater.

Objectives in the site investigations include making an inventory and characterization of springs and gathering field data of infiltration rates and flow rates in springs and rivers at the study area. In the water balance analysis, the objectives are to identify potential groundwater recharge areas and groundwater flow systems communicating with the assessed springs. To evaluate present and past years climate data local to Carrizal is also an important objective to improve the water balance analysis and finding a possible explanation to the recent reduction in spring flow.

1.3 Methodology

Four types of methods were used in this study which are categorised and described in the following sections from 1.3.1 to 1.3.4.

1.3.1 Desktop studies

A theoretical baseline is presented, describing terminology and concepts of groundwater recharge and volcanic geology. Previous studies have covered the local hydrogeology around Carrizal. These studies are reviewed and presented in section 3. Geological layers possibly included in aquifer systems are described with local names and linked to a hydrological conceptual model in the area. Corresponding geological layers were put together based on type of geologic material.

1.3.2 Fieldwork

A fieldwork was conducted during a 5-week period in Carrizal (Costa Rica) with investigations of springs, rivers, and infiltration rates. The original plan of 10 weeks was abruptly aborted because of the global pandemic of Covid-19 leading to travel prohibition. The fieldwork was part of a “Minor Field Study” (MFS) scholarship from the Swedish Board of International Development work (SIDA), which funded the travel and logistical expenses. Tools and equipment were borrowed from the local water organisation ASADA Carrizal (las Asociaciones administradoras de los Sistemas de Acueductos y Alcantarillados comunales), Universidad Técnica Nacional (UTN) and the Division of Engineering Geology at Lund University.

1.3.3 Statistical data analysis

The statistical data analysis includes analyses of climate data and spring flow with both statistical comparison and regression analysis. The data used has been collected by local organisations in Carrizal during several years. Precipitation data was accessed from unpublished reports from *el Servicio de Aguas subterráneas, Riego y Avenamiento* (SENARA, 2020) and flow data was obtained from ASADA Carrizal (ASADA, 2020). These data collections are found in Appendix A.

1.3.4 Water balance analysis

Multiple water balances were made for the study area to quantify groundwater recharge in specific areas and determine types of groundwater flow systems connecting them. The calculations are made up by multiple equations and include parameters from the fieldwork results such as infiltration rates and water flow measurements. Precipitation and spring flow data, same as mentioned previously, were also included in creating the water balance analysis. Calculation methods for each parameter of the water balance can be found in section 4.2.2.

2. Theoretical background

This section brings up the basic theoretical concepts and starts broadly in a hydrological perspective and then narrows down on current scientific understanding of groundwater flow systems in mountainous and volcanic areas.

2.1 Hydrological cycle

The hydrological cycle in Figure 1 shows all the major movements of water on earth and has neither a beginning nor an end. The upward motions, one of many places to start describing the cycle, are directed to the atmosphere, and are caused by evaporation, interception, and transpiration. Water in the atmosphere precipitates, either as snow or rain. When the water returns to the earth's surface again it can flow as runoff, be intercepted by vegetation or infiltrate into the ground. The infiltrated water either percolates down to the groundwater or is taken up by vegetational roots. Groundwater can be stored and transported in aquifers, discharged into surface water or flow in the ground all depending on the geological conditions. And through rivers or by deep groundwater circulation the water finds its way back to the ocean (Narasimhan, 2009).

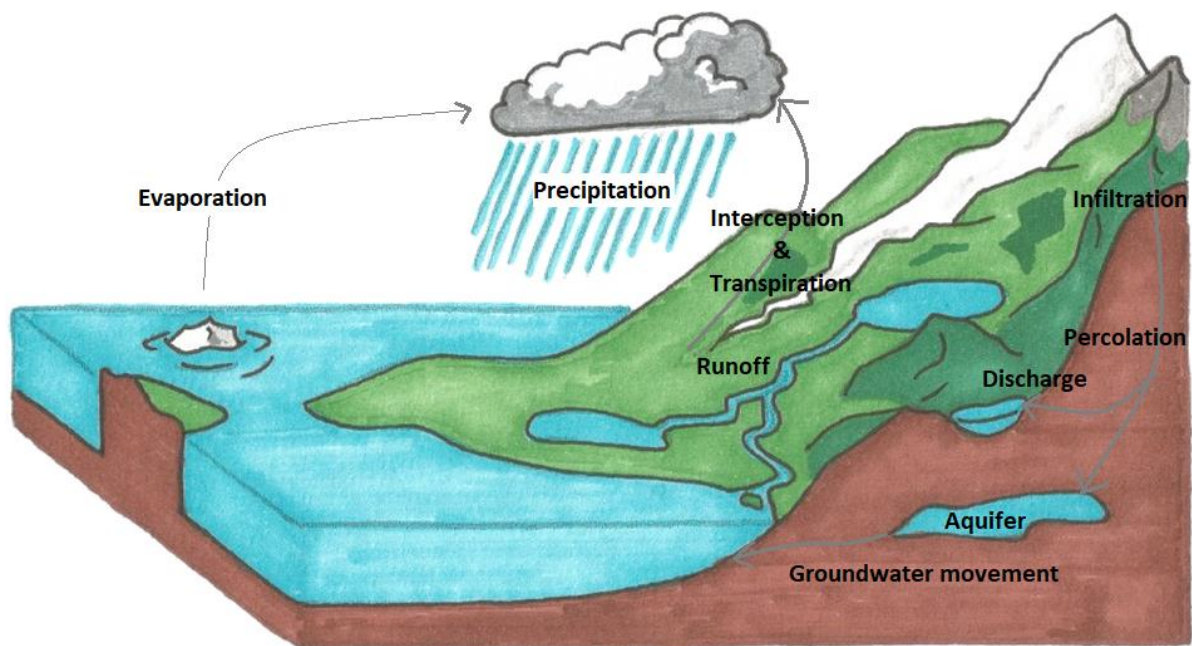


Figure 1. Schematic description of the hydrological cycle.

2.1.1 Groundwater occurrence

Groundwater per definition is all water in the ground filling up pores and fractures in unconsolidated (soil) and consolidated (rocks) geological materials. Storage and transport of groundwater at rates fast enough to extract reasonable amounts for domestic use occurs in permeable hydrogeological units called aquifers. Aquifers can either be confined, unconfined or perched. Confined aquifers have impermeable layers both above and below, while unconfined aquifers only have an impermeable layer below and an upper delimitation called groundwater table. The zone between the ground surface and the groundwater table is called the unsaturated zone. Lastly, perched aquifers are formed by a lens of impermeable material surrounded by permeable material above the water table, causing some water to stay on top of it in an otherwise unsaturated zone. As oppose to an aquifer, an aquitard is a hydrogeological unit which can store groundwater but not transport it (Fetter, 2014).

Groundwater recharge, sometimes referred to as just recharge, is all water reaching an aquifer through infiltration and then percolation. Infiltration in turn, is the process of water entering the unsaturated zone of from the ground surface. Through percolation the water then moves through the unsaturated zone by gravity. The amount of water infiltrating the soil is limited by an infiltration capacity, in other words the maximum rate at which soils, or rocks can absorb water. For dry soils, the infiltration capacity (or *infiltration rate* as a quantitative descriptor) is highest in the beginning of a rainfall event. The infiltration rate then decreases with time as the air pores in the soil are filled with water until a constant infiltration rate is reached; the final infiltration rate (Hargreaves & Merkle, 1998). The final infiltration rate is determined by various parameters such as: vegetation type, geological properties of the unsaturated zone, e.g. grain size, and ground steepness (Huang et al., 2012).

Not all infiltrated water will lead to recharge and some water will leave the unsaturated zone as evapotranspiration, which can be further divided in potential- and actual evapotranspiration. The potential evapotranspiration can be estimated by different empirical correlations, usually based on temperature, percent of daily sunlight or amount of solar radiation, while the actual evapotranspiration is based on measured soil water content. This leads to actual and potential recharge where; *Actual recharge* is the amount of water actually reaching the groundwater table which is quantified by observing the groundwater table over time. *Potential recharge* is just an estimation of recharge by making a water balance from surface water- and unsaturated zone studies (Scanlon et al., 2002).

2.1.2 Groundwater recharge in mountainous areas

There are potentially several flow paths of groundwater in a mountainous area with fast topographical changes and multiple recharge and discharge areas. Theoretically, three types of groundwater flow systems may occur according to Tóth (1963): Local, Intermediate and Regional, see Figure 2. The flow systems are divided by sub-horizontal boundaries where; local flow systems discharge into the nearest river within the same catchment as recharge occurs, intermediate flow discharges in streams or springs at lower altitudes bypassing a surface water divider, and regional flow is the deepest system and does not discharge within the mountainous area. However, the direction of surface runoff may not be the same as that of the groundwater flow at different depths in a mountainous area and delimitation of local and intermediate catchment is not always simple.

Groundwater in the flow systems that ends up in an aquifer in a valley adjacent to a mountain (Valley reservoir in Figure 2) are defined as mountain block recharge (MBR). Circulation depth of the flow systems varies depending on the rock setting of the mountain, fractured crystalline rock areas has deeper circulation patterns than for layered volcanic or sedimentary rock systems generally. The ratio between MBR and discharge on the mountain is not proven to correlate the circulation depth but can improve the ability to predict MBR more accurately. (Markovich et al., 2019)

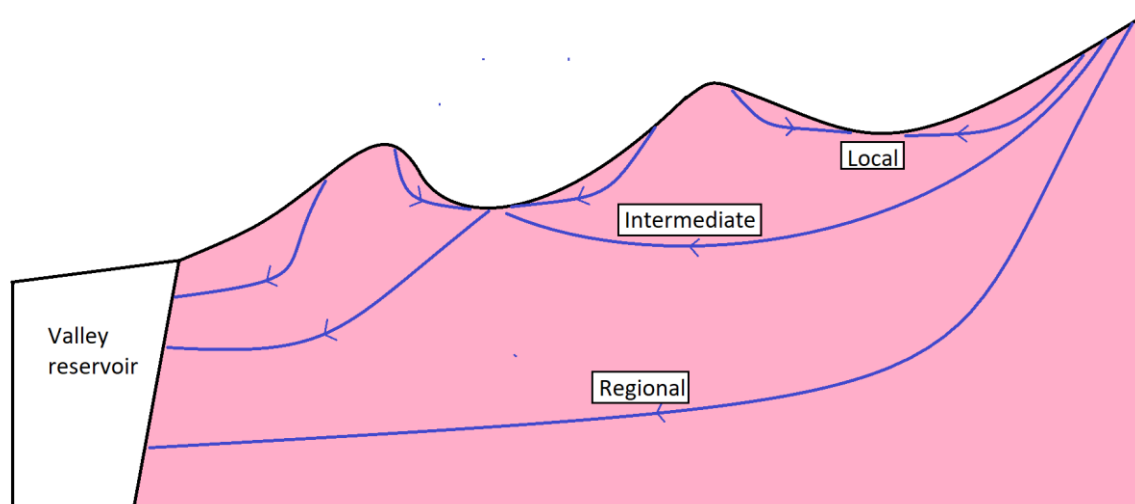


Figure 2. Conceptual view of groundwater flow systems in a mountainous area, modified from Tóth (1963).

2.1.3 Springs

Springs are locations where groundwater discharges at surface level and are formed by different geological conditions in different types of aquifers. In an unconfined porous aquifer **depression springs** can be formed in topographic low points where the groundwater table and surface horizon intersect, creating a local flow system. In a confined- or perched aquifer **contact springs** can be formed in a line of springs at the face of a cliff or in steep slope exposing the multiple layers with different permeability. Other types of springs are **joint springs** or **fractured springs** which forms by permeable fault zones in an otherwise low permeable and fractured aquifer where typically the first type is in lower elevation than the later type. Lastly, **fault springs** are formed by a fault zone that, which in contrast, impedes the groundwater flow and pushes the groundwater table towards the surface in an overlying unconfined aquifer (Fetter, 2014).

2.2 Volcanic geology

There are a few different types of volcanic landforms which have distinct differences in their geological formation and appearance. A **Stratovolcano** has a steeper slope near the top than at the flanks, see Figure 3, due to layers of thick low-viscosity lava closest to the eruption crater while the flanks have more eroded unconsolidated pyroclastic materials. The magma can also diverge from the main chamber creating dikes and if these penetrate all the way to the surface small cones are created on the flanks. (Nelson, 2017)

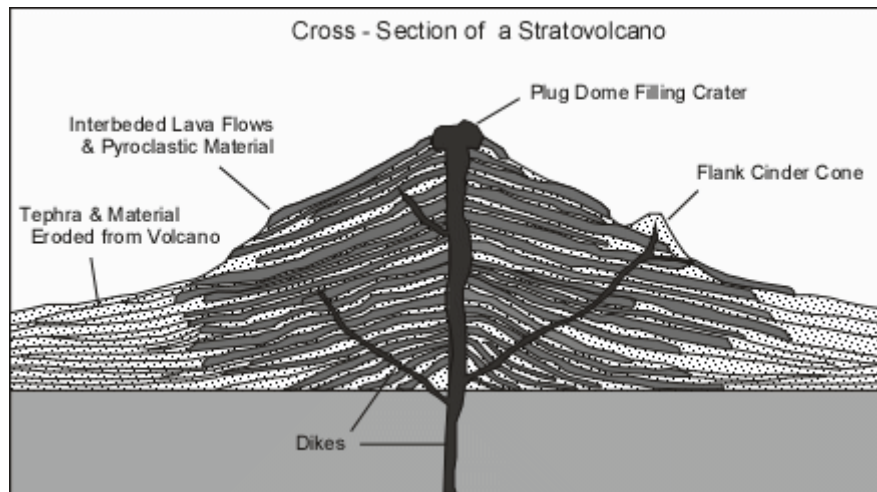


Figure 3. General cross section of a stratovolcano. Source: (Nelson, 2017).

Volcanic rock also called extrusive igneous rock forms by fast cooling magma at a volcanic eruption. The hydraulic properties vary greatly due to chemical composition, structure and how the rock was ejected and deposited. Felsic (rhyolite) lava layers tend to be denser and have a lower permeability if not fractured, while mafic (basalt) lava layers have considerably more connected pores and are normally the most productive aquifer among volcanic rock formations. Basaltic layers are usually thinner and more widespread than andesitic (intermediate lava) or rhyolitic. Different basaltic layers commonly overlap and can be separated by alluvial material or soil zones (U.S. Geological Survey, 2016).

Tuff is a rock formed by compaction and cementation of volcanic ash or dust, it is relatively soft and porous. The appearance depends on the parent material and can be grouped in several ways. Tuff can originate from Precambrian to Recent time but is readily eroded. If hot lava encounters the deposited tuff glassy hardened structure called *Ignimbrite* (welded tuff) can be formed which decreases the permeability (Tuff, 2020)

Volcanic Breccia is a sedimentary rock composed predominantly by angular pyroclastics fragments which is the result from brecciation or emplacement due to volcanic action. In other types of breccia a fine grained matrix is present, however in volcanic breccia this is not always the case (Bowes, 1990).

Andisols is a special type of soil that are found around volcanic areas and has unique properties. The parent material is predominantly weathered tephra, which is permeable and rich in minerals. The permeability favours arability under right topographic and climatic conditions (Andisol, 2011).

3. Description of study area

This section aims to give the reader an introduction to the study area located near Carrizal in Costa Rica. Firstly, 3.1 will cover Carrizal and briefly the surrounding landscape. Secondly, 3.2 will introduce the climate in Costa Rica along with the available weather data. Thirdly, 3.3 will zoom in on hydrogeology on the Barva volcano: Current understanding of hydrogeological characteristics of formations and geological layers. Finally, a hydrogeological profile modified from previous studies close to this study area will be presented in section 3.4.

3.1 Carrizal

Carrizal is located at an altitude of 1440 m a.s.l on the southwest slope of the Barva volcano. The village has roughly 8000 inhabitants in a rural landscape with adjacent cultivated fields of coffee and tomato crops. On higher altitudes, above the village, pastures are more predominant. ASADA Carrizal provides 1500 households with potable water and is part of a national system of local water administrators (Barrantes, personal communication, February 8, 2020). The center of Carrizal lies on a roughly 50 m high ridge alongside two rivers; Rio Quizarrecas and Rio Ahogados, see Figure 4. The study area is covered by the upstream catchments of these rivers and adjacent rivers at the same altitude. ASADA Carrizal extracts its potable water from springs in the area which have individual names: Virgen, Chomorro, Prudencio and Laguna (La laguna in Figure 4). Prudencio has multiple spring outlets and therefore more than one mark on the map indicating the beginning and end of the spring system.

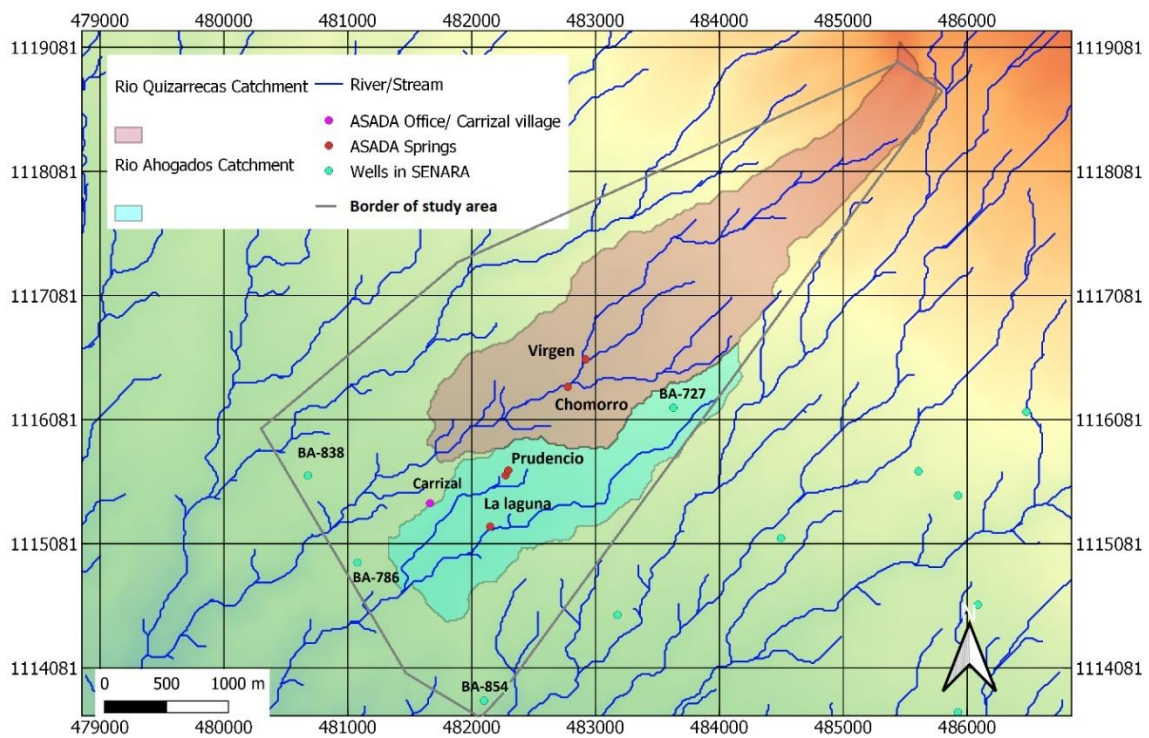


Figure 4. A map of the study area near Carrizal showing the springs used by ASADA, rivers and river catchments made in Qgis and wells registered in SENARA. The coordinate system is CRTM05.

In Costa Rica, Carrizal is located in the Alajuela province while the peak of the Barva volcano is in the Heredia province, see Figure 5. The mountain range in the centre of Costa Rica consist of multiple active volcanos with several peaks above 3000 m a.s.l.



Figure 5. Map of Costa Rica with the village of Carrizal, pink dot, located in the Alajuela province and the peak of the Barva Volcano located in the neighbouring Heredia province. Coordinate system WGS84. Map source: (Gaba, 2008).

3.2 Climate

Costa Rica is a country having various climatic zones. In general, the characteristic Caribbean (east) coast climate is tropical with a lot of rain all year round. The Pacific (west) coast and most of the inland experience a rainy season from May to November, and during the remaining months climate in these areas is mostly semi-arid. The general description is however not valid for all areas, since Costa Rica has also microclimatic zones, which might have a locally specific climate due to rapid topographical changes. Weather data such as temperature, precipitation, humidity, solar insolation et cetera therefore vary a lot spatially within the country.

Daily precipitation data from a weather station, Los Cartagos (located close to Carrizal), can be found in an unpublished report by SENARA (2020) for the years 1968-2019. The average value at this location was calculated to 3580 mm/year. The years 2012-2015 and 2019 had a precipitation amount significantly lower (>15 %) than the mean value, whereas for year 2017 the precipitation was significantly higher than the mean value (>20 %). On a long-term perspective including all years mentioned above, no trend is observed. For these years, the maximum daily precipitation is 190 mm/day, and the total yearly precipitations ranges from 5322 mm to 1980 mm. See Appendix A for more detailed precipitation data.

3.3 Geological setting on the Barva volcano

Large areas of Costa Rica are active tectonic zones and there are several volcanoes in the country. The Barva volcano (peak at 2 906 m a.s.l) is located north of “Valle Central”, the most densely populated region in Costa Rica, and had its last known eruption 500 years ago (Alvarado Induni, 2011). Various geological formations are found on different sides of the Barva volcano, generally ordered in layers and named by distinct different geological characteristics.

The bedrock of the study area near Carrizal is dominated by three formations called Barva, Tiribí and Colima. These formations define the different general hydrogeological layers on the south-southwest side of the Barva volcano. Hereafter in this section, the term Barva will refer to the hydrogeological formation and not the volcano itself. At higher altitudes Colima is located beneath Barva while at lower altitudes the layers of Barva are no longer present and Colima is connected to the ground surface, which is a common feature of layers on a Stratovolcano. Tiribí is only found between the Barva and Colima formations. The more permeable layers of the formations are explained by fractured andesitic and basaltic bedrock. Wells and springs in the area have reported flows between 60 and 375 litres per second (Arias, 2014).

The stratification of geological layers in Barva and Colima are shown in Figure 6 on the next page. The thickness of each layer in the figure is an approximation and only in relative scale to the other layers, but also varies in different parts of the formations. Barva consists of the following layers (ordered in descending depth); Los Ángeles, Bambinos, Porrosati and Carbonal, and Bermúdez (Losilla Penón, 2010). Barva covers an area of 275 km² but all layers are not present everywhere. Individual features of each layer in Barva along with the features of the formation Tiribí and Colima are described in following paragraphs.

The top layers Bambinos and Los Ángeles are only found at higher altitudes and are closest to the surface in Barva. The layer Los Ángeles only exists in the eastern part of Barva and has not been found nearby Carrizal. Bambinos consists of overlapping lava flows in the northwest-southeast direction containing porphyritic andesites with visible phenocrystals which characteristically are 6-8 mm. The lava flows in Bambinos contain autoclastic gaps both in the bottom and on the top of the formation and have a maximum thickness of 100 metres (Arredondo, 2011). Bambinos consists of elongated hills in the southwest direction. A part of this top lava layer is documented at a village 2 kilometres northwest of Carrizal and is described as massive lavas of andesitic composition. The groundwater pattern of Bambinos and Los Ángeles can be described as perched aquifers, rapidly discharging water

into springs and recharged by direct precipitation. The general flow direction of the surface water is from northeast to southwest in Bambinos (Losilla Penón, 2010).

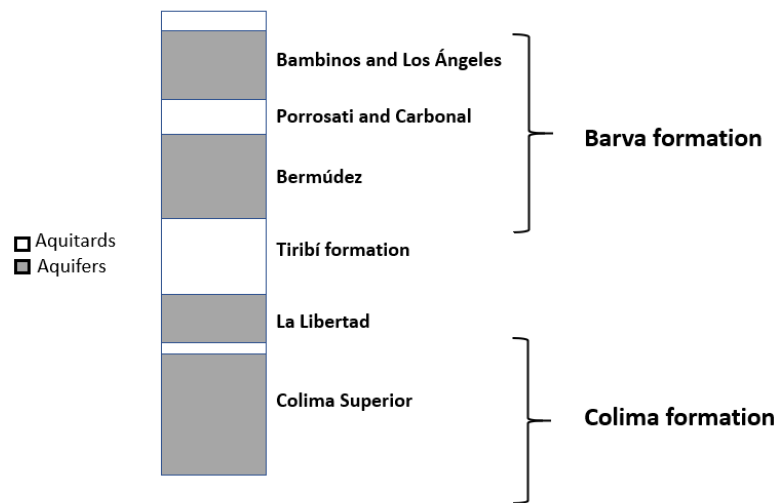


Figure 6. The general stratigraphy of aquifers around the Barva volcano. Grey color indicates aquifer and white color indicates aquitard. The thickness of each layer is only relative to each other in this figure.

The layers La Libertad and Colima Superior are located below Barva in the Colima Formation. Both consist of fractured andesitic lava and are separated by a thin aquitard. Colima Superior and La Libertad can be described as a system of perched aquifers (Ramírez, 2007). The layers described in this section with the corresponding geologic material and thickness are found in Table 1 .

Table 1 The different layers in study area with corresponding formation. Geologic material and thickness are also shown.

Formation name	Layer name	Geologic material	Thickness
Barva formation	Bambinos	Andesitic and basaltic lava	10-100 m
Barva formation	Porrosati	Volanic sands and clay tuff	20 m
Barva formation	Bermúdez	Lava	< 50 m
Tiribí formation	-	Pyroclastic material	45-150 m
Colima formation	-	Andesitic lava	> 100 m

The layers Porrosati and Carbonal are located beneath Bambinos. Porrosati and Carbonal are mostly made of pyroclasts, forming large aquitards which separate the aquifer of Bambinos from Bermúdez. At some places “tobácea” (tuff) is found. Carbonal contains lahars and other epiclasts around the border to other layers. The thickness of the layer is estimated to 20 metres (Protti, 1986).

The layer Bermúdez consists of fractured lava and is located below Porrosatti and Carbonal. The transmissivity of this layer is reported to 400 m²/day and the maximum thickness is 85 m, thus Bermúdez can act as an aquifer (Protti, 1986). Its thickness depends on the water level, which is influenced directly by precipitation. The water age in Bermúdez was determined from Tritium tests to be 10-15 years (Gomez, 1987). Typically, the layer Bermúdez has very large fluctuations in water level. The water level is decided by the season and there is a complex recharge-discharge relationship with the rivers (Gomez, 1987). The same study also reports 3 recharge mechanisms: percolation from upper aquifers or aquitards, direct infiltration from precipitation and infiltration from rivers and streams.

The formation Tiribí is an aquitard containing pyroclastic material. Its thickness varies between 45 and 150 m. The layer covers an area of approximately 500 km² (Ramírez, 2007).

3.4 Previous hydrogeological studies near Carrizal

Based on lithology from three wells close to the study area, a previous study (Losilla Penón, 2010) has created a stratigraphic conceptual model of aquifers- and aquitard. The locations of the three wells BA-838, BA-786 and BA-854 can be found in Figure 4 and the stratigraphic conceptual model is found in Figure 7. Two deeper valleys can be seen in the topography of this model, where the river Rio Quizarrecas flows in the left one and the river Rio Ahogados in the right one. Looking on the horizontal axis from the left in Figure 7, the valleys are located at 400m and 1200m respectively. There is a ridge between the two river valleys which is the same ridge as Carrizal is located on.

Based on the description and stratification of the geologic layers in section 3.3 the two light green layers in Figure 7 are most likely Bermúdez and Bambinos. The top yellow layer is Porrosatti and Carbonal while the second yellow layer is the Tibirí formation. The brown top layer is andisol (soil) and the deepest dark green layer is part of the Colima Formation.

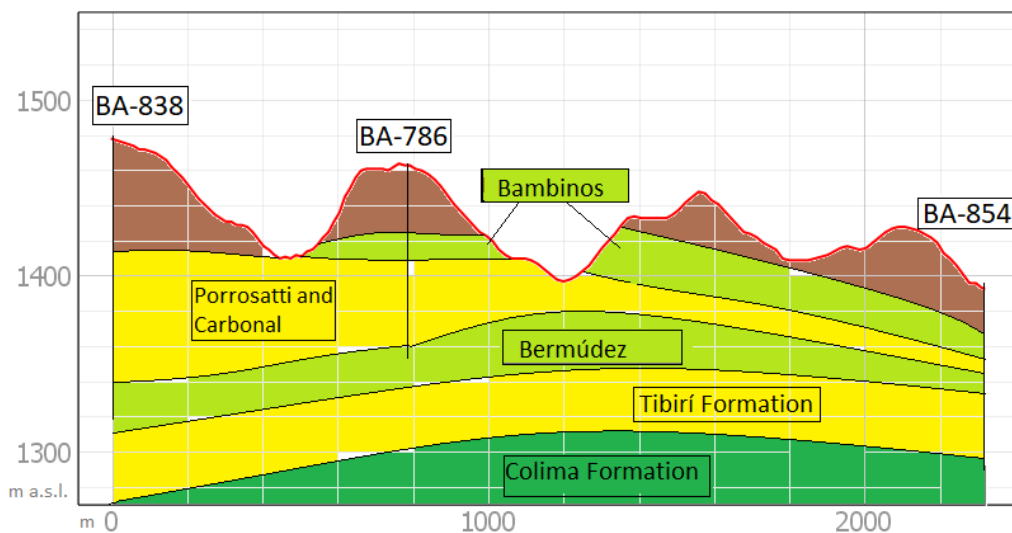


Figure 7. A cross section profile of aquifers and aquitards close to Carrizal, the unit on the vertical axis is m a.s.l and the unit on the horizontal axis is in meters. Green colours indicate different aquifers, yellow aquitards, and brown is for soil deposits. The figure is made after a stratigraphic conceptual model of aquifers- and aquitard by Losilla Penón (2010).

4. Methods

The methods for this master thesis are divided in two parts, the first part is the fieldwork conducted in Carrizal, Costa Rica. The second part is more analytical and uses available data collected by organisations and previous studies in Costa Rica in addition to the collected data from the fieldwork.

4.1 Site investigations and measurements

4.1.1 Ocular assessment of springs

The first week in Carrizal was spent finding as many springs as possible in the study area. The original plan was to locate springs registered at *Sistema Nacional de Información Territorial* ([SNIT](#)). This information turned out to be mostly misleading. Instead, knowledge from locals, farmers and workers at ASADA Carrizal had to be used to find spring locations in the study area.

Each spring is documented according to the five following characteristics: flow discharge angle, slope, volume of flow, geological particle size and locations relative to nearby streams. These characteristics are selected from an integrated spring classification system by Springer and Stevens (2009). This type of characterization can give an indication on which type of groundwater flow system a spring is connected to (local, intermediate or regional), but also serves the purpose of describing the kind of springs that will be used in the water balance analysis for future comparability reasons.

4.1.2 Infiltration

To measure infiltration rates in the study area, a double-ring infiltrometer was used (Johnson, 1963). The technique uses two large metal rings for measuring how fast water is infiltrating into the ground. The outer ring prevents horizontal flow and is constantly filled up with water. Inside the inner ring the water surface level is sinking and is measured repeatedly for two hours and filled up between measurements if needed. Figure 8 below shows a visual representation of the setup when it is installed below ground surface to reach further down into the unsaturated zone. Measuring water surface level inside the inner ring and calculating the cumulated infiltration can be used to estimate vertical hydraulic conductivity with the help of infiltration models.



Figure 8. Setup of a double-ring infiltrometer below ground surface.

There are various infiltration models available to estimate the vertical movement of water in the soil. Some models are *empirical models*, e.g. Horton's Equation, while Philip's equation is a commonly used *physically based model* (Or et al., 2018).

Philip's equation was chosen for estimation of hydraulic conductivity in this study because there is a commonly used correlation between the model parameters and the hydraulic conductivity. The model is based on the solution of Richard's equation, cited in Or et al. (2018, p. 116). The model equation is found in Equation 4.1 and expresses the movement of the top surface of a water body moving into the soil as a function of time:

$$I(t) = S_0 * t^{0.5} + A * t \quad \text{Equation 4.1}$$

$I(t)$ is the cumulative infiltration measured in the double ring infiltrometer (mm), t the time (min), S_0 the sorptivity ($\text{mm}/\text{min}^{0.5}$) and A a constant (mm/min). The first term describes the sorptive forces of a relatively dry soil. The second term is the contribution from gravity. The relative effects of gravity compared to sorptivity is higher for longer times, or when the soil becomes more saturated (Or et al., 2018). Equation 4.1 is valid for shorter times but for longer times the vertical infiltration needs to be modelled as an infinite series in powers of $t^{0.5}$.

Data points of cumulative infiltration $I(t)$ versus time (obtained from the double-ring infiltrometer experiment) can be fitted to the parameters in Equation 4.1. To obtain the equation parameters S_0 and A , a GRG-Nonlinear optimization algorithm for minimizing the sum of the squared distances between the model points and the collected data is used. The vertical hydraulic conductivity (K) can then be calculated from the model parameter A , with the correlation in Equation 4.2 found by (Fodor et al., 2011):

$$K = \frac{3A}{2} \quad \text{Equation 4.2}$$

4.1.3 Flow measurements in rivers and springs

Two methods of measuring flow are “jug and stopwatch” and *velocity-area* (Brassington, 2017). These are suitable for measuring different kinds of water flows and were used in separate measurements in this study, one for measuring spring flow and the other for river flow.

Spring flow is measured with “Jug and stopwatch” which is a simple method that requires only a bucket and a stopwatch. The bucket size should be chosen suitable to the magnitude of the flow. A short and wide bucket is preferred to a tall and narrow one, to make sure the whole jet is caught in the bucket. The stopwatch is used to measure the time it takes for the bucket to fill up. By knowing the time and volume, the flow can be calculated as litres per second.

River flow is measured with the *velocity-area* (Brassington, 2017) method which requires simple tools such as measuring tape, a stopwatch, and a floating object. Figure 9 shows a visual explanation of the parameters d , b_1 and b_2 (d and b are the distance and width of the river section). The floating object is released at the beginning of the section and a stopwatch measures the time for it to travel to the end. This is repeated five times to reduce random errors. The velocity can then be calculated by distance divided by average time (t_{av}). This method overestimates the river velocity since the surface velocity is higher than the mean velocity. Therefore, a multiplier of 0.75 is added on the calculated velocity. The widths and corresponding depths are used to calculate a rectangular cross-section area. The river’s width is measured at two locations perpendicular to the flow direction (b_1 and b_2). For each width, the average depth is calculated (y_{av}). From the variables and assumptions explained above, Equation 4.3 calculates the flow volume Q [l/s]:

$$Q = 0.75 \cdot \frac{b_1 y_{1,av} + b_2 y_{2,av}}{2} \cdot \frac{d}{t_{av}} \quad \text{Equation 4.3}$$



Figure 9. The parameters b_1 , b_2 , and d shown visually, note that the endpoints of the section d do not necessarily have to coincide where the stream width is measured.

A rectangular cross-section is assumed for two reasons. Firstly, the water flow was extremely low at the time of measurement. Secondly, this assumption does not necessarily increase or decrease the area compared to a triangular or trapezoidal cross section.

4.2 Data analyses

Both methods described in this section use the previously collected data from the two unpublished reports by SENARA (2020) and ASADA Carrizal (2020) together with parameters from the fieldwork.

4.2.1 Statistical data analysis

The statistical data analysis mainly compares the flow rates of four springs used by ASADA Carrizal (2020) with precipitation from a nearby weather station (SENARA, 2020). Flow measurements of the springs were collected only once a month by ASADA but are considered as an average for the whole month in this study. The analysis will be in two parts: one focusing on monthly comparison, and the other on annual.

The monthly comparison is made by plotting spring flow and precipitation over time. By observing maximum and minimum values of precipitation and comparing it with significant shifts in spring flow rates the following months, a travel time of groundwater from recharge to discharge can be estimated. Precipitation and spring flow rate patterns are also a key feature of evaluation which can contribute to a better knowledge of groundwater flow behaviour.

Total annual precipitation shows a great variation at the study area, for the compared years, ranging from 2525 mm in 2019 to 4643 mm in 2017 (SENARA, 2020) which is why a monthly comparison may not be enough of an investigation. An annual comparison using linear regression of three different scenarios is therefore suggested as a method of investigating annual correlations. The intentions are to find a correlation between yearly average spring flow and total annual precipitation. The three scenarios are as followed; 1: yearly average spring flow vs. total annual precipitation, 2: yearly average spring flow vs. total precipitation from two consecutive years, 3: yearly average spring flow vs. total precipitation from three consecutive years.

4.2.2 Water balance analysis

A water balance consists of all the inputs and outputs of water in a catchment, which includes both water on the surface and in the ground. A general equation of a water balance is found in Equation 4.4 (Fetter, 2014):

$$P - Q - E_T = \Delta S \quad \text{Equation 4.4}$$

P = Precipitation

Q = Runoff

E_T = Evapotranspiration

ΔS = Change in groundwater storage

When ΔS is positive, the groundwater is recharged. Discharge from springs in the study area is mainly used for extraction but needs to be considered in the Q term of water leaving the catchment. Q can then be separated in two terms, one for river runoff (Q_R) and another for spring runoff (Q_S). Measurements of flow in rivers and of some springs are only available at the time of the conducted fieldwork, the remaining months are simulated based on a fraction of flow from a nearby ASADA-springs with all year-round values. Groundwater flow systems of intermediate, or regional water discharge can influence ΔS if present but are not quantified individually in this method.

A water balance also needs to be defined to a specific region where inputs and outputs occur at the borders and surface of the region. SAGAs toolbox in QGIS can calculate watersheds with the input data of a digital elevation model (DEM). A method in this software is “Multiple Flow Direction” (Freeman, 1991) which calculates direction of surface water runoff. In a fast changing topographic landscape the runoff water could flow more or less straight towards a main river or stream channel. More divergent flow paths are therefore chosen to not be part of the catchment to minimize the risk of creating a catchment that does not contribute to local groundwater flow systems.

The springs Virgen, Prudencio, Chomorro, and Laguna have monthly flow data collected for several years (ASADA, 2020) and are therefore chosen as focus points with individual water balances in the analysis. The whole river catchments of Rio Quizarrecas and Rio Ahogados are not used as borders for the water balance analysis due to limitations in river flow measurements.

4.2.2.1 Infiltration calculations

Two methods of quantifying infiltration are performed in this study. The first infiltration method (Equation 4.5) assumes neglectable surface runoff from precipitation and simply calculates the infiltration from the net precipitation:

$$I_1 = P - E_T \quad \text{Equation 4.5}$$

where I_1 stands for infiltration, P for precipitation and E_T for evapotranspiration.

In Equation 4.5 the evapotranspiration E_T is calculated as the potential evapotranspiration E_{Tp} multiplied with the fraction of days which has precipitation each month. An assumption is made here that the potential evapotranspiration occurs on days that has precipitation, and no evapotranspiration occurs when on days with no precipitation due to fast infiltration rates. Hence, it is assumed that on days when evapotranspiration occurs, the potential (maximum) evapotranspiration occurs. There are various models available to estimate potential evapotranspiration. Available weather data made it suitable to use the empirical correlation by Blaney and Criddle (1950) cited in ONU (1972) for estimating the potential evapotranspiration:

$$E_{Tp} = (8.10 + 0.46 * T_{av}) * R_s \quad \text{Equation 4.6}$$

In Equation 4.6 T_{av} is the average monthly temperature and R_s is the average monthly percent of daily sunlight. The monthly value of the fraction of days with precipitation for the year 2017 will be used for all years. Variation in number of days with rain is assumed to influence the infiltration only marginally.

The second approach is based on a method in Schosinsky and Losilla (2000) which uses evapotranspiration and infiltration coefficients from empirical studies in Costa Rica (Equation 4.7). This method estimates that generally 12% of the rain in Costa Rica either evaporates or gets intercepted by vegetation foliage. An infiltration coefficient (C) estimates how much of the remaining precipitation that will infiltrate, leading to the following equation:

$$I_2 = 0.88 \cdot C \cdot P \quad \text{Equation 4.7}$$

C is calculated from Equation 4.8, sum of three governing parameters. K_{FC} is the infiltration contributed from soil texture, K_V the infiltration from vegetation cover, K_P the infiltration from the slope.

$$C = K_P + K_V + K_{FC} \quad \text{Equation 4.8}$$

The fraction of infiltration affected by vegetal cover (K_V) in Equation 4.8 can be estimated depending on the type of land use and tabulated values are found in Schosinsky and Losilla (2000). Huang et al. (2012) showed that the infiltration rate and the soil moisture after a rainfall event first increased slightly with increasing slope, but decreasing for slopes greater than 16%.

In Schosinsky and Losilla (2000), an empirical equation (Equation 4.9) based on the final infiltration rate of the soil was obtained. The authors claim that this empirical equation is valid for Costa Rica. The empirical equation expresses the fraction that infiltrates by soil texture (K_{FC}) as a function of the final infiltration rate F :

$$K_{FC} = 0.267 \cdot \ln(F) - 0.000154 \cdot F - 0.723 \quad \text{Equation 4.9}$$

The final infiltration rate (F), in Equation 4.9, is the steady state condition of infiltration and can be obtained from the infiltration tests and model parameter A in Equation 4.1. It should be added that the methodology of Schosinsky and Losilla (2000) does not take into consideration that the infiltration rate is higher in the beginning of a rainfall event.

Change in groundwater storage is calculated as the sum of flows entering the saturated zone minus the sum of flows leaving the saturated zone over a time period. This change can be seen as the potential recharge. The two different methods of infiltration calculations can be used in calculating ΔS as following:

$$\Delta S_1 = I_1 - Q_S - Q_R \quad \text{Equation 4.10}$$

$$\Delta S_2 = I_2 - Q_S - Q_R \quad \text{Equation 4.11}$$

The term Q from Equation 4.4 is divided into Q_S and Q_R , where Q_S is spring water flow and Q_R is other discharge from the unsaturated or saturated zone. I_1 originates from Equation 4.5 and I_2 from Equation 4.7. Equation 4.10 and Equation 4.11 are the final equations that will be used for calculating yearly ΔS values to determine if each catchment can support a local flow system for the ASADA springs or not.

5. Results and discussion

This section shows results from measurements and observations made in Carrizal. The covid-19 pandemic outbreak had a severe impact in the planned field activities, shortening the time of fieldwork. The limited collected data is complemented with an extensive review of the available literature on the area's geological setting. Fieldwork data was complemented with data previously collected by other organisations. The analyses of the more extensive data are presented in section 5.2 and 5.3. Finally, different result parts will be tied together in section 5.4 with a conceptual model of groundwater flow system extending across the study area.

5.1 Fieldwork

Fieldwork results cover three investigations: ocular assessment of springs, double-ring infiltration measurements and flow measurements in springs and rivers. The measurement points were registered with GPS and are presented in Figure 10. Rivers and the two catchments, in the same figure, are created in QGIS with a DEM, 12X12 m pixel resolution, obtained from a local supervisor in Costa Rica. The coordinate system used is local to Costa Rica and called CRTM05. ASADA springs have individual names and are visualized differently in Figure 10 than non-ASADA springs found at the study area. Laguna and i4 share the same coordinates and overlap (see Figure 10).

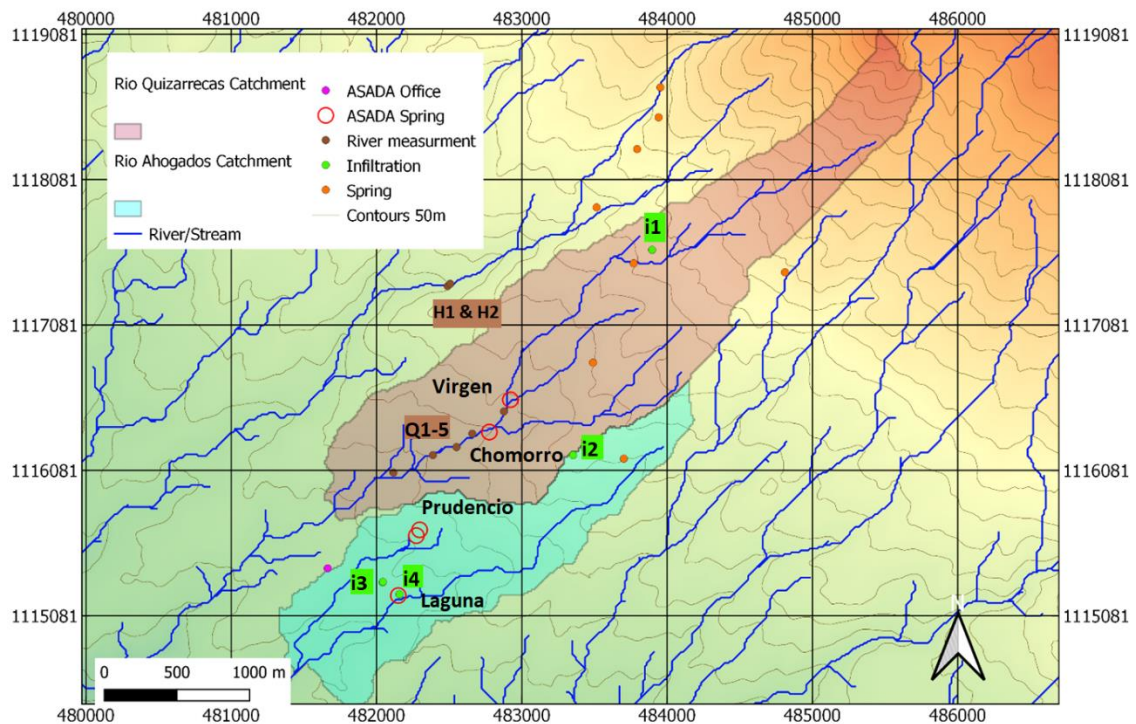


Figure 10. Overview map with locations of fieldwork measurements. "H1 & H2" and "Q1-5" are river measurements with numbers in ascending order from upstream to downstream. Four locations of infiltration measurement correspond to i1, i2, i3 and i4. Springs are differentiated by ASADA and non-ASADA springs, with individual names on ASADA springs.

5.1.1 Springs

The ocular assessment of springs includes 17 springs in total, 14 of these are additional to the ASADA springs. The result is compiled in Table 2 with two intervals for each characteristic to showcase major types of differences in springs at the study area. Boundaries for each characteristic's interval and how many springs there are within each interval are also shown in Table 2. Individual information about each spring's characteristics can be found in Appendix B.

All the springs that were found in the study area are used for water supply, by farmers or landowners, and have constructed protection around the outlet. This protection made it difficult to further investigate the angle of discharge and is therefore left out from the results. At some spring locations the slope was difficult to judge due to surrounding obstacles. The general approach became to judge the average steepness between a few meters above and a few meters below the spring. Flow measurements were only possible at 14 out of 17 springs in the study, therefore there are only 14 springs included in C₃ (Table 2).

Table 2. Compilation matrix from the Ocular assessment. C = characteristic and n=number of springs. Only 14 springs are represented in C₃.

Characteristics	Interval boundaries	n	Interval boundaries	n
C ₁ Vertical distance from nearby major stream or river	0–5 m	10	>5 m	7
C ₂ Slope at spring eruption	Gentle (<45°)	10	Steep (>45°)	7
C ₃ Water flow	Low (< 4 l/s)	11	High (>4 l/s)	3
C ₄ Visible blocks and stones next to the spring	Yes	15	No	2

All springs with a gentle slope are within five meters vertically from a nearby stream, except one, while all springs with a steep slope are more than five meters away from a nearby stream. The ASADA spring Chomorro has the characteristics of steep slope and more than five meters to a stream and can be seen in Figure 11 on the next page. Springs in the lower interval of C₁ are sometimes found in dried up riverbeds where there has potentially been more flow in the past or other periods of the year. C₃ and C₄ are more random compared to other characteristics and no clear patterns can be found between them nor with C₁ or C₂.

The variety of spring characteristics found in the study area indicates on springs formed by different geological conditions. The volcanic geology with layers of high permeable fractured lava and low permeable layers in between makes the springs found on steep slopes and sometimes in series likely to be contact springs. However, since the flow rate does not show any clear pattern with any other characteristic it is hard to connect them to the same aquifer and flow system, without more information. The human interferences at the springs also makes it harder to predict the natural causes and forming processes.



Figure 11. Picture of the spring Chomorro with Jacob Sannum climbing and ASADA Carrizal worker supervising.

It is possible that more natural springs could have been found if the fieldwork had been conducted in the wet season May-December since all springs found in the study area are used for supplying water for human consumption or irrigation. It is of interest to see how much the results would change and if more springs can be found depending on the time of the year a fieldwork is performed and compare the result to see seasonal differences.

5.1.2 Infiltration

The Double-Ring Infiltrometer was used at 4 locations, see Figure 10. In total, seven infiltration tests were conducted, with one or two tests at each location. Data points from the infiltration tests are fitted to Equation 4.1 to retrieve the model parameter A, which is the parameter the vertical hydraulic conductivity is calculated from (see Equation 4.2). Curves obtained from data fitted to Equation 4.1 are found in Figure 12, Figure 13 and Figure 14. Hydraulic conductivities are found in Table 3 along with location, depth, and accuracy of the fitted model. For the tests conducted below soil surface, the obtained model parameter A is used in the water balance to estimate the fraction of infiltrated precipitation.

At two places (Coffee 2 and Grass 2), the instrument was also dug into the ground to compare infiltration rates above and below the soil surface. Results at i1 exist only at 0.63m depth since no flat enough surface could be found in the forest areas, which made it impossible to conduct an accurate measurement at surface level.

Table 3. Calculated hydraulic conductivity for all the infiltration experiments and corresponding location. The map point column shows the names of the point on the map (see Figure 10). The R squared value for the data fit is shown in the far-right column. For three tests the model parameter A is shown.

Map point in Figure 10	Name/land use	Depth below soil surface [m]	Model parameter A [m/d]	Vertical hydraulic conductivity [m/d]	R ²
i4	Coffee 1	0	2.12	3.18	0.99
i4	Coffee 2	0.76	1.23	1.84	0.99
i3	Coffee 3	0	0.03	0.05	0.99
north east of i4	Coffee 4	0	1.35	2.03	0.99
i2	Grass 1	0	5.51	8.26	0.99
i2	Grass 2	0.85	1.49	2.24	0.99
i1	Forest 1	0.63	8.33	12.5	0.99

For the forest vegetation type, the calculated hydraulic conductivity is significantly higher than for the other vegetation types. This infiltration test at 0.63 m below the surface in the forest yielded a higher value even compared to the tests at agriculture and grass land use areas at the soil surface. The location of the test in the forest is on steep soil with observed high organic content – hence high permeability. The influence of slope is not considered in the calculation of hydraulic conductivities but is in the infiltration calculation for the water balance and is therefore worth mentioning.

In Figure 12, the experiment data is plotted at three locations as a scatter plot. These three datasets all have in common that the Double-Ring Infiltrrometer was set up below the soil surface. In Figure 12, the fitted line for Equation 4.1 is also shown for the three locations. For the next figures, only the fitted curve without the scatter plot of measured data is shown. The R-values in Table 3 are convincing enough that the fits are good ($R > 0.99$ for all cases). The model parameter A is the final infiltration rate. This parameter is equal to the slope of the fitted curve as time grows to infinity. To visually observe a high final infiltration rate, the slope of the fitted curve between approximately 100 and 120 minutes is used. It is obvious that the forest had a significantly higher final infiltration rate compared to other land uses in Figure 12. The forest transports water 5-6 faster than the other vegetation types at this depth (see hydraulic conductivities in Table 3).

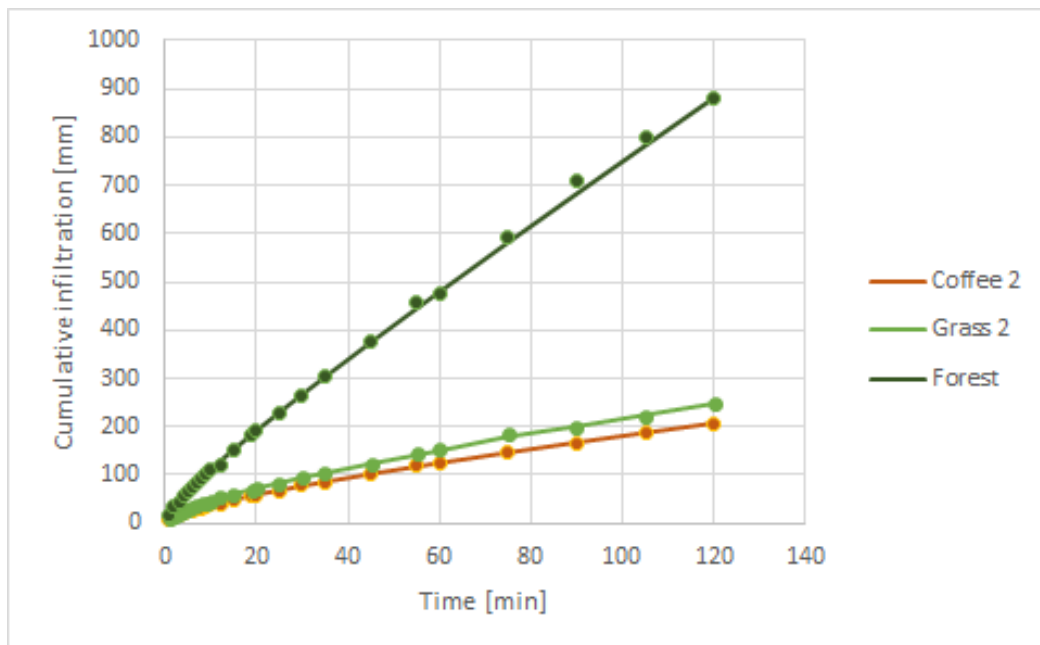


Figure 12. The fitted cumulative infiltration curves of Coffee 2, Grass 2 and Forest (i_4 , i_2 and i_1 in Figure 10), plotted to compare the infiltration on different land uses (below soil surface). The scatter plot is the actual data points of each land use.

The experiments on the land uses of Coffee and Grass are compared both at ground surface (Coffee 1 and Coffee 2) and below ground surface (Coffee 2 and Grass 2). Field measurement data is not shown in Figure 13 and only the fitted model curve). It is observed in Figure 13, both below the soil and on the ground comparing the two land uses, the grass had a higher final infiltration rate. Although, in the beginning of the experiment, Coffee 1 had a more rapid increase than Grass 1 in the first few minutes. This higher rate in the beginning of the experiment is reflected in the sorptivity (the model parameter S_0 in Equation 4.1). Indeed, Coffee 1 showed a sorptivity of $32 \text{ mm}/\text{min}^{0.5}$, whereas Grass 1 showed a sorptivity of $15 \text{ mm}/\text{min}^{0.5}$. The prior has higher sorptivity than the latter – i.e. when the soil is dry, it attains more water if higher sorptivity. Similar argument can be used for Figure 14 when comparing Coffee 2 and Coffee 3, a higher final infiltration rate does not necessarily correlate with higher or lower sorptivity.

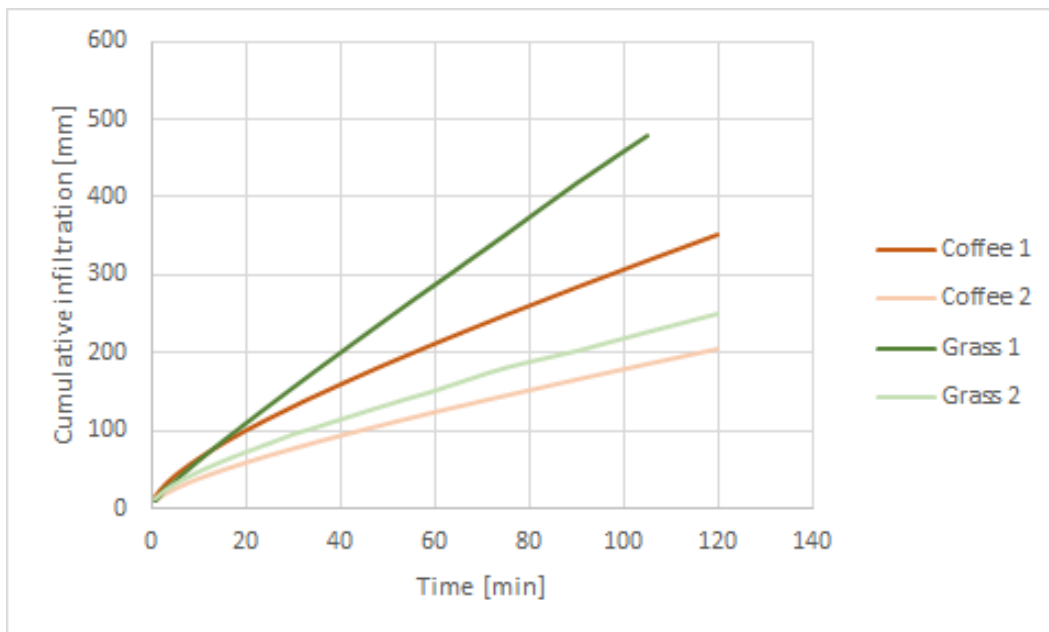


Figure 13. Fitted models of cumulative infiltrations at locations with coffee plantation and grass covered fields.

The infiltration experiments for the land use “Coffee” were conducted on the same plantation, but on different altitudes. Altitudes not to be confused with the different depths Coffee 1- and Coffee 2 tests were conducted at. The tests were both conducted downhill, right on the border of the coffee plantations. Coffee 3 and Coffee 4 were conducted at surface level in different places, but more uphill compared to Coffee 1 and Coffee 2 (less than a hundred meters difference in altitude). All Coffee infiltration experiments took place within a radius of one kilometre in the same coffee plantation; the plot of the fitted curves with Equation 4.1 is shown in Figure 14. Comparing the experiments occurring on top of the soil, Coffee 1 (experiment most downhill, i4 in Figure 10) shows a higher final infiltration rate than Coffee 3 (i3 in Figure 10), thus a higher vertical hydraulic conductivity. No clear pattern for the sorptivity could be observed when going from downhill to uphill.

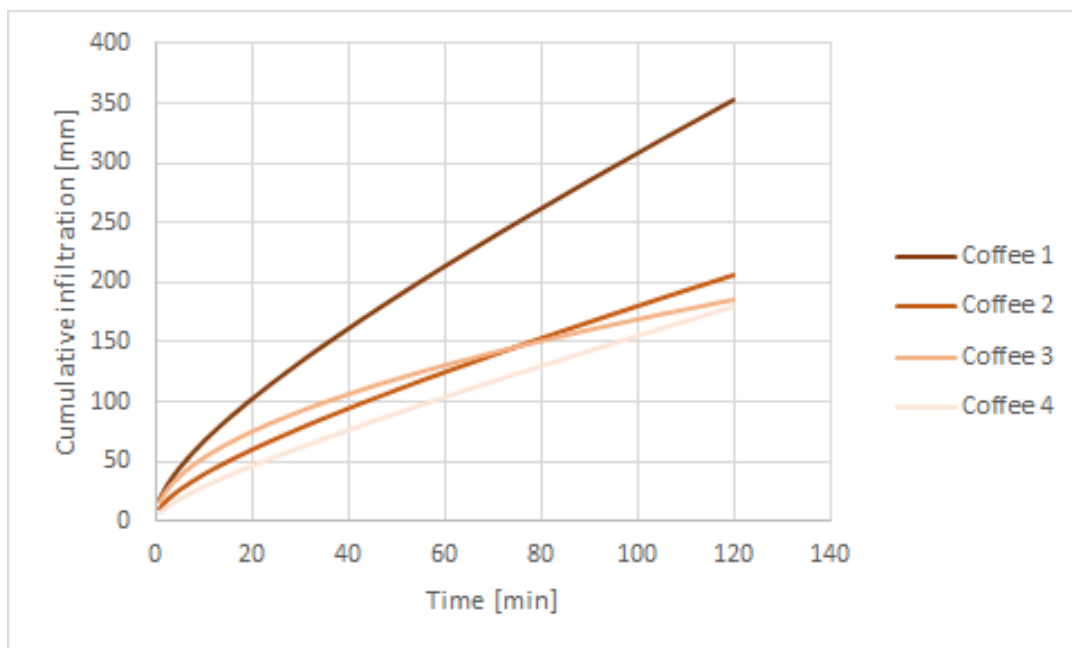


Figure 14. Fitted models of cumulative infiltrations at multiple locations on a coffee plantation.

For the study area, there might be a spatial variability of vertical hydraulic conductivity correlating with the altitude. Generally, there is a steeper slope higher up on the volcano which can enhance the infiltration rate (Huang et.al, 2012). Coffee 3 shows significantly lower conductivity values compared to the other Coffee experiments. The local soil characteristics and the local flow paths might be more relevant for the different conductivity values and a heterogenous unsaturated zone can create local variations in hydraulic conductivity.

Distance to the groundwater table and thickness of the unsaturated zone are factors which might influence the infiltration measurements, which will influence the calculated hydraulic conductivity. Coffee 3 was conducted approximately ten meters from a mud road. Cars driving there regularly may consolidate the soil which increases the bulk density. Different local water flow paths of the unsaturated zone are possibly explaining the very low conductivity. This distance was thought to be sufficiently far away from the road.

Coffee 4 (Figure 14) shows a rather linear increase of infiltration (rather constant infiltration rate) through the whole experiment, speculating that the test time was too short here. Similar pattern can be seen for Forest in Figure 12.

The highest precipitation for one day (maximum daily average rainfall intensity) between year 1968 and year 2016 was 0.19 m, as explained in section 3.2. In the water balance, only infiltration experiments done below soil surface were considered to estimate the amount of precipitation infiltrated. Looking at the subsurface experiment values in Table 3, all values of final infiltration rates except one exceeds the maximum rainfall intensity of 0.19 m/day in the study area, i.e. the maximum tolerable final infiltration rate (vertical hydraulic conductivity) before runoff occurs is not exceeded. Although looking at even shorter time scales, there could be even higher rain intensities, hence this is not enough to conclude that no runoff occurs. But the runoff is surely limited. In Schosinsky (2006), the threshold of a vertical hydraulic conductivity where all water infiltrates for soil is used as 1568 mm/day, i.e. roughly 1.6 m/day. This threshold is reached for all the subsurface experiments, implying that theoretically surface runoff never occurs. Looking at all infiltration tests (on soil surface and subsurface), Coffee 3 is the only test where the threshold was not reached. The conclusion is that there might be locally less permeable soil but generally most of the precipitation will infiltrate.

The calculated hydraulic conductivities for the study area can be validated and compared with values from a global data source in the software called Soil Grids. Soil Grids is a system which generates soil properties based on global soil profile data and machine learning algorithms (ISRIC – World Soil Information, 2020). For the location of the infiltration site Grass 2 on 0.85 m depth, soil properties of andisols from this database were used. From the bulk density and from the mass percent clay, silt and sand, a saturated hydraulic conductivity value was obtained through the database Rosetta (Rosetta Commons, 2003). Rosetta is a program implementing a Pedotransfer Function, i.e. it is designed to estimate hydraulic properties from soil data. The hydraulic conductivity obtained from the Pedotransfer Function (1.34 m/day) is rather similar to the value obtained from the physically based infiltration model (2.24 m/day). Considering these findings, it seems reasonable to assume that vertical percolation through the top andisol layer might be a possible pathway to recharge the aquifer.

The result from the infiltration tests shows that the hydraulic conductivity changes with the type of land use. The recharge of groundwater could therefore be affected by a change in the local land use, for example if forest or grassland is turned into agricultural fields. The vertical hydraulic conductivity for agriculture land use (Coffee 2) in Figure 12 is lower than the other locations, speculating that the general pattern could be lower infiltration occurring when natural landscape is turned into agriculture, thus possibly lower recharge.

5.1.3 Rivers

5.1.3.1 General observations

During the fieldwork in February-March 2020 the rivers and streams were investigated, some of the streams and rivers were completely dry as seen in Figure 15. Dry streams are found more commonly higher up in the catchments but are not absolute for a certain altitude. Where the 2 streams join at the spring Virgen, seen in Figure 10, the western channel had no flow while the eastern had flow during the fieldwork. The dry western stream was investigated thoroughly far up in the catchment and only one spring was found near it, which is used for extracting water for a local landowner.



Figure 15. Stream above Virgen with no flow in Mars 2020

The particle size and presence of river sediments are observed to be changing greatly in the study area. The types of material vary rapidly and are changing in sections with boulders and stones all the way to parts with finer material such as sand or clay. At a few places higher up in the catchment outcrops are also observed.

The vegetation along Rio Quizareccas, Rio Ahogados and nameless connecting streams also changes. In some parts the whole width of the river was found to be densely covered with small bushes while other parts were totally bare. The canopy cover did however not change, and highly dense vegetation was almost always present on the slopes adjacent to the streams and rivers. On the ridges between the rivers: vegetation was much less dense, and conditions were dry compared to the humid river valleys.

5.1.3.2 Flow data

Flow velocities were measured at seven locations in two different rivers, see Figure 10. The calculated flows for each measurement and river are displayed in Table 4, where the measurement number increases from upstream to downstream. The altitudes are displayed in a shifted altitude scale, where the relative altitude is zero at measurement number 1 and decreasing into the negatives at the following measurement points downstream. The measurements of flow were made during a single day for each river and due to a forced early departure from the fieldwork no measurements in river Ahogados were conducted.

Table 4. River flow measurements and their relative locations

River	Measurement number	Relative altitude [m]	Distance from first measurement [m]	Flow [l/s]
Quizarrecas	Q1	0	0	3.8
Quizarrecas	Q2	-36.2	305	5.5
Quizarrecas	Q3	-40.8	449	16.6
Quizarrecas	Q4	-66.8	618	7.5
Quizarrecas	Q5	-101.5	917	0.7
Honda	H1	0	0	1.3
Honda	H2	-33.4	23	2.2

The spring Chomorro is located along Rio Quizarrecas between Q1 and Q2, but its water did not reach the river due to extraction and did not influence the river flow at the time of measuring. The generated channels representing streams and rivers in Figure 10 are not always correct which was observed at the connecting stream near Chomorro during the fieldwork, the stream is actually joining Rio Quizarrecas after the spring and Q2. The connecting stream is what causes the major increase in flow between Q2 and Q3, which is otherwise hard to understand from observing the map in Figure 10. Different maps of the area were compared, and the location of this stream shifted between maps and could possibly be from a fast-changing landscape or recent urban development.

A 55% decrease can then be seen from Q3 to Q4 and no visible human interferences between these measurement locations were observed. Downstream Q4 farmers were extracting water for irrigation and damming up the river. At this part of the river more finer materials and less boulders were observed. Downstream Q5 the river flows close to urban areas and small farms where tubes and pumps were observed, bad odour of possible sewage was smelt at this location.

In the river Honda, which is to the northwest of Rio Quizarrecas, there is an 41% increase in flow between the two measurement points. Due to the rough vegetation and terrain only two flow measurements were made at this location. This section of the river had large boulders and a hissing sound of a potential underground flow at a certain place between H1 and H2.

A few measurement points, where no joining rivers or human interference disturbed the flow, could be used to interpret the connectivity of the riverbed and adjacent groundwater. Large variations in flow between some of the locations indicate a diffusive rate that shifts from positive to negative in different parts of the river. These shifts make it hard to predict what type of groundwater flow systems a high-altitude river is connected to. Inflow to the aquifer can therefore qualify as indirect recharge from parts in the river with decreasing flow.

With the measurement conducted only in the dry season the results could possibly change if river flows are measured at another time of the year due to large seasonal changes in precipitation at the study area. The behaviour of water moving between river and aquifer can potentially be driven by groundwater storage and repeated data collection at different times of the year could increase understanding of groundwater flow systems in the study area.

5.1.4 Summary of fieldwork results

The fieldwork results can be summarized into a key message from each section:

- Protective constructions made it difficult to identify what geological conditions formed the springs and specific flow systems can not be determined without more information.
- High infiltration rates are found in all land use areas tested, although 4-6 times higher in forest than on coffee plantations.
- The river *Rio Ahogados* shows large fluctuation in flow at different locations. In some sections, the fluctuation was neither explained by human impacts nor adjoining streams. A possible explanation is an interplay between river and groundwater, but further investigations is needed to confirm the quantities.

5.2 Statistical data analysis

5.2.1 Monthly comparison

The monthly comparison was made with only two springs, Virgen and Prudencio, and is shown in Figure 16 and Figure 17. The flows vary greatly, between 0-80 and 3-40 l/s respectively in the given years. The other two ASADA springs, Chomorro and Laguna, had little variation in flow, see Appendix A, and were therefore not used in this comparison.

In the period 2016-2017 the flow and precipitation vary a lot, peaks in precipitation come in different months each year but generally in May-December. The fastest increase in spring flow occurs in September – October both years, even if the accumulated rainfall is greater in 2017 right before these months. The pattern of spring flow rate changes between the two years in Figure 16 and responses to a monthly precipitation of the same magnitude vary. It is important to remember that the measurement of spring flow rates was only conducted once a month, which day is not recorded, and precipitation can occur on any day within a month, this decreases the accuracy of interpretation of the graphs somewhat.

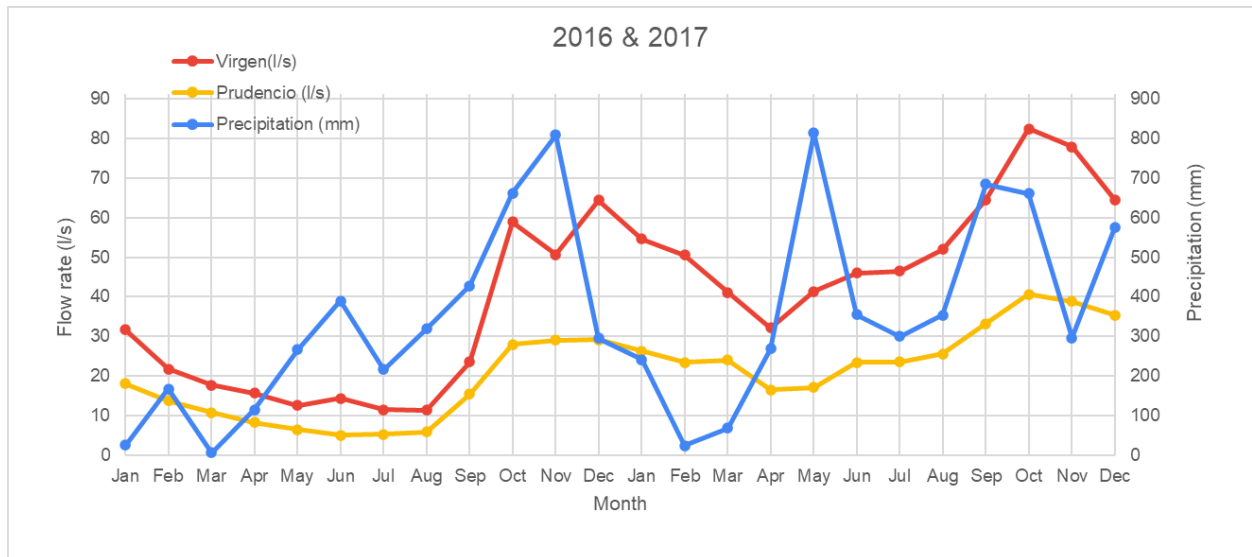


Figure 16. Plotted graph with flow and precipitation from the years 2016 and 2017

Figure 17 shows that there are small changes in precipitation patterns between the years of 2018 and 2019 but also compared to the years in Figure 16. There are some differences in magnitude of the precipitation peaks while the months where precipitation peaks occurred are more or less the same in all years. The pattern of spring flow rates also changes from year to year, some years have greater and more stable flow rates while other years have lesser and more fast shifting flow rates.

Comparing the two springs, the flow rate in Virgen seems to respond faster to an increase or decrease in precipitation than in Prudencio which has less fluctuation with longer rise and fall periods. After several precipitation peaks, Prudencio shows a peak or sharp increase in flow rate within 3-4 months while Virgen does the same within 0-1 months, these events in both springs are however more apparent when the flow is low. A shorter travel time and a more local groundwater flow system for Virgen than Prudencio can be one explanation. The measurements of flow once a month are a reliability to predict the groundwater travel time and higher resolution of data is needed to improve the result.

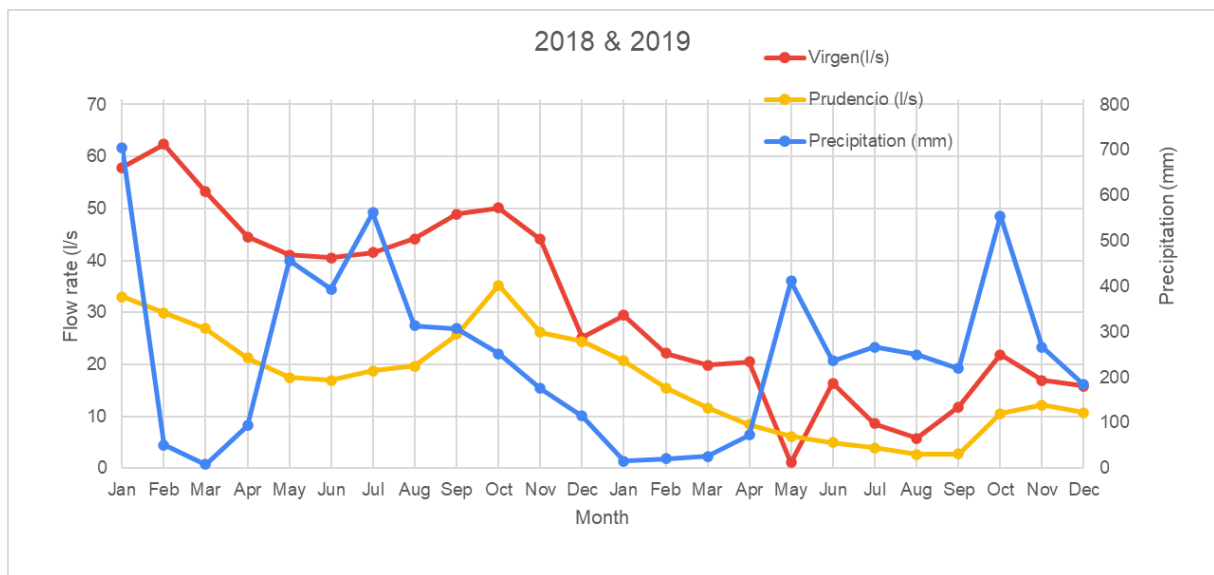


Figure 17. Plotted graph with flow and precipitation from the years 2018 and 2019

5.2.2 Annual comparison

Results of the annual comparison consist of three scenarios where each year's average spring flows are plotted versus different number of years accumulated precipitation. The three scenarios are as followed; 1: yearly average spring flow vs. total annual precipitation, 2: yearly average spring flow vs. total precipitation from two consecutive years, 3: yearly average spring flow vs. total precipitation from three consecutive years. Scenario 2 can be seen in Figure 18 and the dotted line represents the regression equation made to match the flow values for each spring and year, scenario 1 and 3 can be found in Appendix C.

The steepness of the regression equations, denoted "linear" in Figure 18, tells how much the yearly average spring flow increases per mm precipitation. In scenario 2 visualized below, Virgen has a steeper regression equation than Prudencio and is therefore more sensitive to precipitation, which can be correlated with the faster responses mentioned in the monthly comparison. Laguna and Chomorro have small flowrate variations in absolute values. These are hard to see when put on the same scale as flows from Prudencio and Virgen and are therefore on a secondary axis Figure 18.

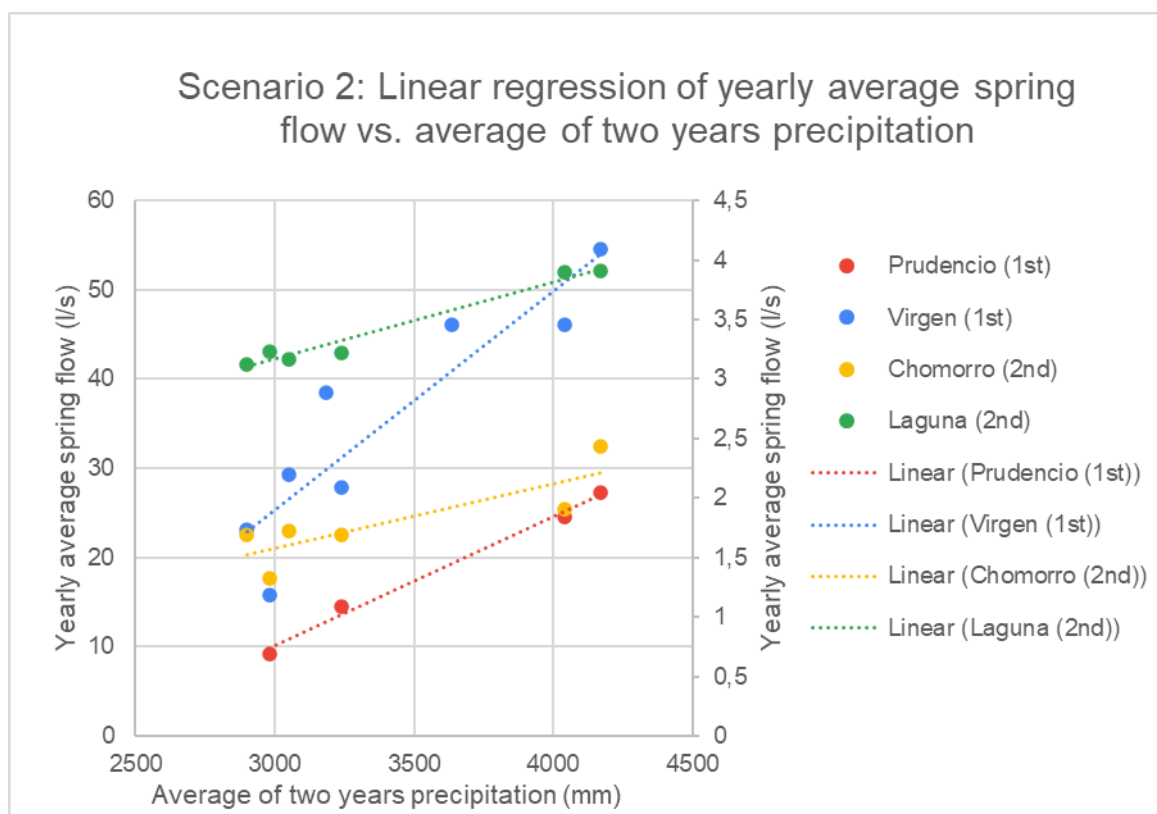


Figure 18. Linear regression of yearly average spring flow in the four ASADA-springs versus average of two years precipitation, scenario 2. 1st or 2nd indicates primary or secondary vertical axis.

The amount of data points varies between the springs, Virgen has the most years of collected data and Prudencio the least in all scenarios. The amount of data could influence the accuracy and significance of the regression analysis, fewer data points could give a false high significance. It is also possible that a regression other than a linear relationship could be suitable for the analysis, but with limited amount of data the simplest form of regression was motivated.

A R^2 value was calculated to see how well the plotted line of a linear equation fits with the data points. The best fits of linear regressions for all the springs are found Scenario 2, see Table 5. Spring flow in Chomorro exhibits the lowest correlation with precipitation in all the scenarios which could mean that it is less dependent on amounts of precipitation and somewhat controlled by other factors. However, the significances are high enough in scenario 2 to assume that precipitation is the main limiting factor of spring flow in all springs.

The large variation in yearly precipitation shows a significant effect on the total amount of water coming out from the springs within 1-2 years and a travel time of groundwater in the area longer than this is therefore not probable. The recent reduction in flow rate in the ASADA-springs can therefore be explained by this statement since the years of 2018 and 2019 show less precipitation than the average.

Combining the best fit of the linear regression (Scenario 2, 0-2 years of precipitation) with the response time in the monthly comparison (0-4 months), a potential water age of discharging water from the ASADA springs is estimated to range from 0-24 months. This means that precipitation from one month is affecting the springs flow rates both in the coming months and in less noticeable scale, the amount of spring discharge in the year after. The large range of 24 months is most likely due to widespread recharge areas, both near and far from the spring locations in the oblong river catchment. The estimation of water age can probably be more accurate with higher resolution of flow data combined with accumulation of precipitation in shorter periods or to give the yearly values statistical weight.

Table 5. Significances of regression analysis from different scenarios of the four assessed ASADA-springs. The three scenarios are 1: yearly average spring flow vs. total annual precipitation, 2: yearly average spring flow vs. total precipitation from two consecutive years, 3: yearly average spring flow vs. total precipitation from three consecutive years.

R^2	Virgen	Prudencio	Chomorro	Laguna
Scenario 1	0.591	0.646	0.504	0.825
Scenario 2	0.818	0.992	0.693	0.968
Scenario 3	0.474	0.416	0.167	0.785

5.3 Water balance analysis

The sub-catchments used in the water balance analysis are delimited from watersheds generated in QGIS which can be seen in Figure 19, the area of each sub-catchment is shown in Table 6. Higher values on the legend in Figure 19 indicate areas of less divergent surface water flow paths towards a given coordinate close to each ASADA spring. Chomorro and Virgen have overlapping watersheds and only a flow path ratio of 7.2 or higher was chosen to calculate the sub-catchment area.

Inside the catchment connected to Virgen lies two non-ASADA springs and one river which have flow measurements from the fieldwork. These two springs and single river have simulated values for the remaining months included in the water balance analyses.

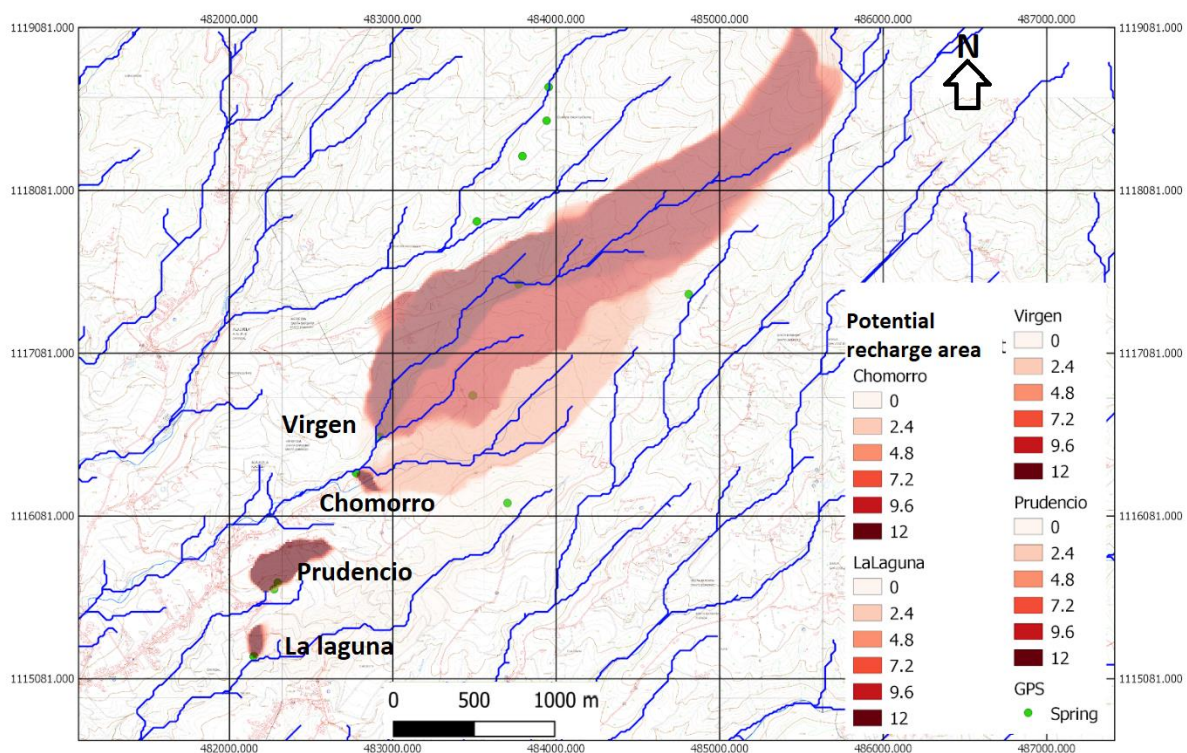


Figure 19. Four watersheds created by the method “Multiply Flow Direction” in QGIS based on Freeman (1991) Higher values in the legend indicates a more direct flow path towards a given coordinate.

Table 6. The sub-catchment areas for each spring.

Spring name	Sub-Catchment area [km ²]
Virgen	2.14
Prudencio	0.09
Laguna	0.02
Chomorro	0.01

Values of E_T can be found in Table 9 in Appendix A along with the climate data used for the calculation. The climate data contain values of average temperature and daily sunlight which were collected by a weather station in Costa Rica. As mentioned in section 2.1.1, actual evapotranspiration should be estimated as the potential evapotranspiration times the current water content divided by the water content at field capacity. Because no data of field capacity and no precise unsaturated zone thickness, the actual evapotranspiration was calculated by the specific approach explained in section 4.2.2.

The model parameter A from Equation 4.1 (values in Table 3) was used as input in Equation 4.9 to estimate the infiltration I_2 . For each catchment, values of K_V and K_{FC} in Equation 4.8 were chosen according to the major land use in corresponding catchment. See Appendix C for all parameters used in the calculations of I_2 (Equation 4.7). Monthly values of storages S_1 and S_2 (Equation 4.10 and Equation 4.11) were calculated for all four sub-catchments and then aggregated to yearly values. The yearly average values between S_1 and S_2 , denoted ΔS , for each year with available spring flow data are the main result for the water balance analysis, found in Table 7.

Quantification of deeper groundwater flow systems is not part of the water balance, and the value of S can probably not be treated as the actual storage of groundwater for each sub-catchment. The value of S is mainly used as a basis for discussing the groundwater flow path nearby and between each ASADA-spring sub-catchment, rather than speculating about the actual amount of water storage accumulated over several years.

Table 7. Yearly ΔS (Change in groundwater) for the four sub-catchment linked to ASADA springs, the value is calculated as the average between ΔS_1 in Equation 4.10 and ΔS_2 in Equation 4.11.

Year	ΔS (10^4 m³) at Virgen	ΔS (10^4 m³) at Prudencio	ΔS (10^4 m³) at Laguna	ΔS (10^4 m³) at Chomorro
2012	270			
2013	320			
2014	370		-0.48	-7.0
2015	350		-0.89	-6.9
2016	510	-21	0.93	-6.8
2017	580	-53	0.47	-8.0
2018	380	-54	-0.27	-9.2
2019	330	-13	-0.24	-8.1

For Virgen, the value of ΔS is positive in all the years included in the study. One explanation is that large volumes of water might percolate down to a deeper aquifer. Water could also leave the catchments as groundwater, flowing below surface water dividers if aquifer layers extend that far.

For Prudencio, the value of ΔS are negative for all years; the inputs of water do not make up for the continuous flow leaving the spring. Schosinsky (2005) suggested that Prudencio might be fed from a nearby river. This is not included in the calculation but could be interpreted from the results. A negative ΔS would indicate that there is a net discharge of water from the aquifer, rather unlikely to occur consequently for several years, hence there must be a source of incoming water other than precipitation in the local sub-catchment.

For the spring Laguna, ΔS was relatively close to zero for all years. It is the only spring investigated where ΔS is shifting between positive value and negative value for different years. The water feeding this spring is probably from an isolated local groundwater flow system closely correlated to precipitation changes.

For Chomorro, no clear pattern between ΔS and precipitation could be observed. Although a possible explanation for ΔS being negative all six years could be that the catchment of Chomorro is underestimated. Another explanation is that Chomorro could be fed by intermediate flow paths from another catchment or from nearby rivers where no measurements were conducted.

The study area in this report generally has high slope, thus it is highly unlikely that a significant increase in ΔS is a long-term effect, which aligns with the prediction, made in 5.2.2, of a general water age between 0-24 months in the ASDA-springs. The precipitation volume is regulated by the catchment area, which is generated from the DEM in QGIS. The DEM has an accuracy of 12x12 metres and since the catchment areas are relatively large, this resolution should not serve a reason to estimate ΔS wrongly. Water extracted from wells or rivers was not modelled in the water balance, only spring extractions were, which could influence the result of S positively.

A positive ΔS for a catchment in an upstream area with high slope could be interpreted as having multiple groundwater flow systems as outputs. While a negative ΔS can be interpreted as the opposite; groundwater coming as an inflow from adjacent basins. In Figure 7 it was shown that the Bambinos layer extends below a surface water divider (between 600 m and 1000 m on the horizontal axis), connecting two basins. This permeable layer could transport water between the basins, possibly as intermediate flow mentioned earlier in the section about Mountain Block Recharge. The system of connective layers feeding the different springs is hard to map out in its entirety. Fractured bedrocks which are common in tectonic active areas could also increase the connectivity between deeper and older lava layers acting as aquifers, thus reducing the intermediate flow and adding to the regional. To confirm the hypothesis of more fractured lava layers in certain areas further investigations are needed.

The two infiltration calculation methods were compared for the Virgen sub-catchment. The ratio between the two infiltration values I_2 and I_1 were calculated for each year. The average ratio I_2 / I_1 for these years was 1.26 and the standard deviation of the ratio was 0.12. These values suggest that Equation 4.7 (I_2) estimates the infiltration higher than Equation 4.5 (I_1). For I_1 it was assumed that all net precipitation infiltrates, but this assumption did not lead to a greater value of infiltration compared with I_2 .

The standard deviation of the yearly ratio (0.12) suggests that generally it is most likely that Equation 4.7 is very likely to estimate a higher infiltration ($1.26 - 0.12 > 1.00$). Although in our results, ΔS for all years is far from zero, which indicates that the difference in the estimation of infiltration is not causing large uncertainties.

To give a perspective of ΔS in relation to the size of sub-catchments and precipitation, the storage is showcased in the unit m per year in Table 8. Even though a lot of water is extracted from the spring Virgen, ΔS in its sub-catchment is relatively high and almost half of the precipitation infiltrating in this area does not discharge within the delimited catchments. Which means that there probably are water leaving the saturated zone each year through deeper groundwater flow systems which has not been quantified in this study.

For Prudencio and Chomorro, ΔS is very far from zero some years. Therefore, water not quantified in this study is probably entering the aquifer from somewhere else. Perhaps from Rio Quizarrecas or the sub-catchment of Virgen. For Laguna, ΔS is very close to zero all four years. It is the only spring where the storage is shifting between positive value and negative value for different years (Table 8). Seasonal assumption in this water balance could have a large effect on the result, and data covering the whole year at specific locations, e.g. flow measurements in the rivers, would most definitely increase the accuracy of this method.

Table 8. The change in water storage for four years in the unit meter per year.

Annual ΔS in m/year	Virgen	Prudencio	Laguna	Chomorro	Precipitation (m/year)
2016	2.4	-2.5	0.4	-6.2	3.7
2017	2.7	-6.2	0.2	-7.3	4.6
2018	1.8	-6.4	-0.1	-8.4	3.4
2019	1.5	-1.5	-0.1	-7.4	2.5

5.4 Conceptual model of groundwater flow systems

The conceptual model of groundwater flow systems is presented in both Figure 20 and Figure 21, where Figure 20 focuses on the area in close proximity to the ASADA-springs while Figure 21 extends the whole study area and shows the geographical location of Figure 20. The different groundwater flow systems presented in the model are in the form of Local, Intermediate and Regional. The groundwater flow systems depends mainly on ΔS in the local sub-catchment around each spring seen in Table 7, but also on the altitude changes.

Information from previous studies and lithology from nearby wells are used to further explain which aquifer layers that could belong to which groundwater flow system but are not visualized in the model since the depth and thickness of these layers are unknown in most parts of the study area. The conceptual model presented in Figure 20 is perpendicular to the profile in Figure 7 and the flow systems can possibly be linked to the different aquifer layers Bambinos, Bermúdez or Colima seen there. The water age of groundwater in the Bermúdez aquifer layer is 10-15 years (Gomez, 1987) and therefore not likely connected to the ASADA springs. Bambinos are closer to the surface and can potentially be connected to the ASADA springs with Intermediate and some local flow systems with the potential water age of 0-24 months.

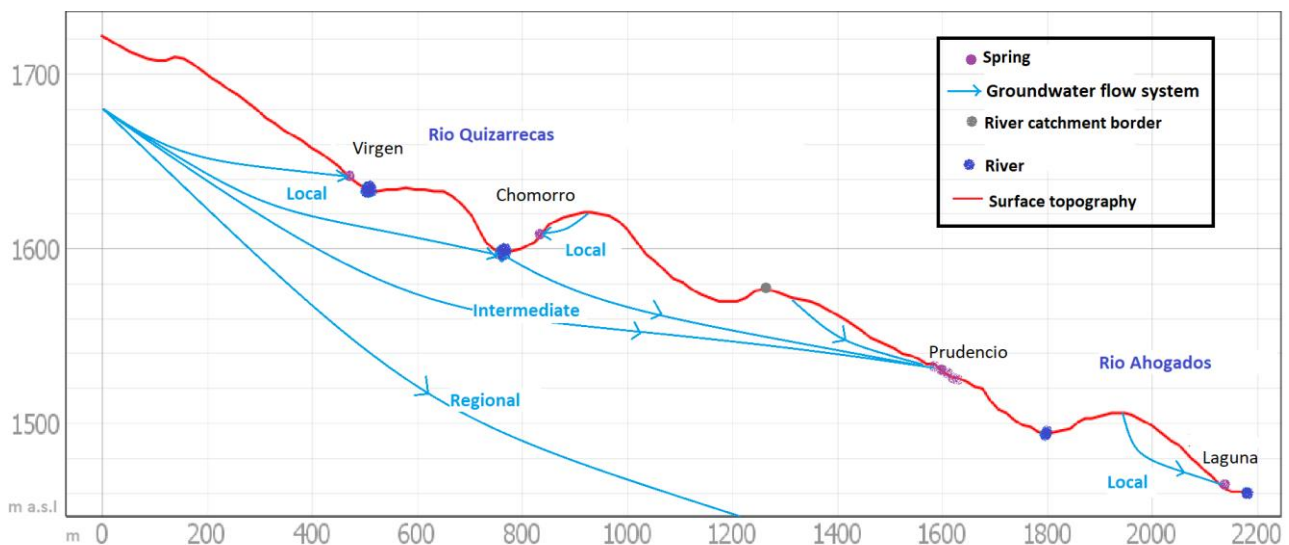


Figure 20. Conceptual model of groundwater flow systems in the study area connected to the ASADA springs. For location of this profile, see Figure 21.

The infiltration tests indicate that water infiltrate the ground at any type of land use in the study are due to high vertical conductivities in the soil layer. However, it is not clear if or where the infiltrated water percolates to an aquifer layer and at which depth the different flow system is at. With no geophysical measurement or groundwater levels it is hard to conclude exactly where the transport of water takes place. Local and Intermediate flow systems are likely to occur in aquifer layers closer to the surface which can both be closed or open with the presented volcanic stratigraphy and connected to the stream and rivers in the area. Regional groundwater flow is more likely to occur in closed aquifers deeper down preventing the water from discharging at higher altitudes and therefore not connected to the springs.

The well BA-786, located below the study area, has lithology records of more impermeable layers than the well BA-727 which is located at the same altitude as Virgen, drilling reports from the two wells can be found in Appendix D. The less impermeable lithology could explain the result from the water balance near Virgen which shows that there is much more water infiltrating at this high altitude than what leaves the same sub-catchment at surface level. On the other hand, more impermeable layers seen in BA-786 can possibly explain the isolated local flow systems in the lower altitude sub-catchments. Further investigation on the extent of geological layers in the area is needed to confirm this.

The Regional and Intermediate groundwater flow systems, seen in Figure 21, is a possible explanation model to balance out the continuous large positive ΔS in the upstream catchment. Especially with the result of a potential water age of 0-24 months in consideration, which means that groundwater will not stay in the same catchments for long periods of time. To confirm how much these deeper groundwater flow systems will contribute to MBR more downstream discharge locations need to be investigated and included in the water balance analysis. Flow systems between the rivers, Rio Ahogados and Rio Quizareccas, could perhaps be more detectable in the rainy season when there are flow in more parts of the rivers and streams.

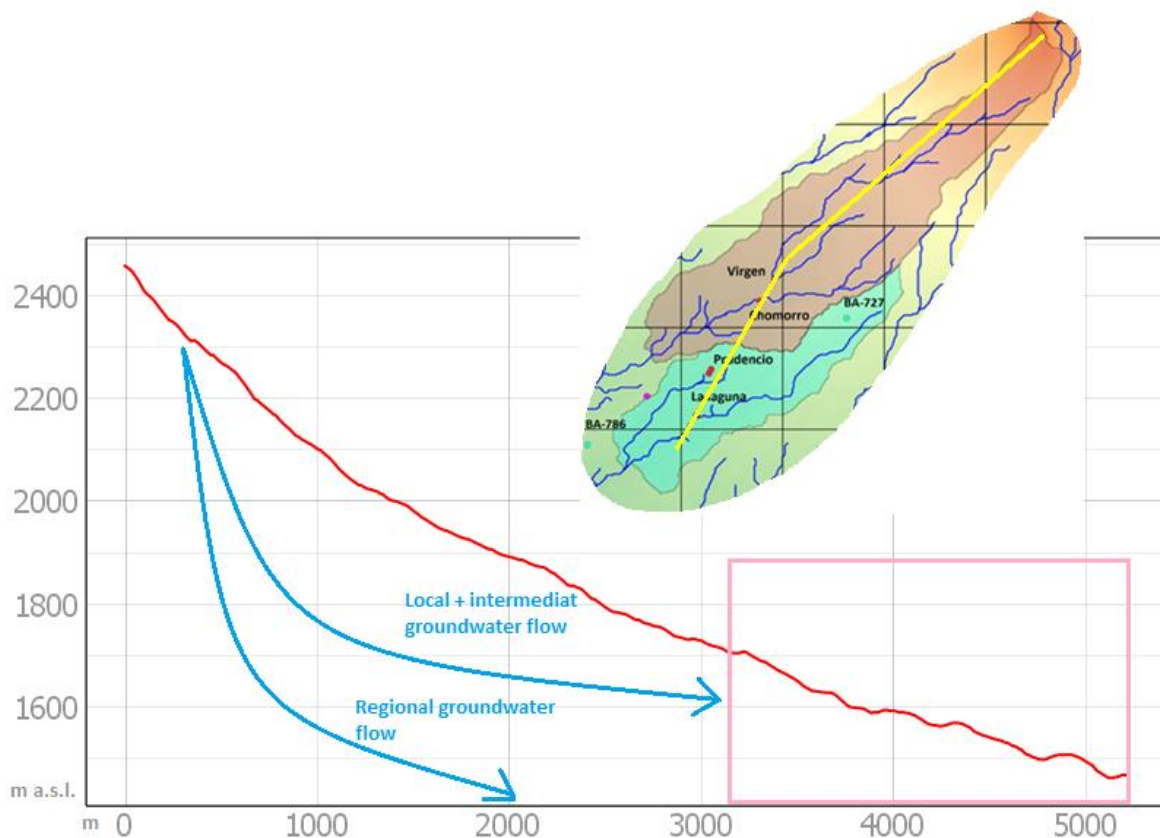


Figure 21. Ground surface altitude with conceptual groundwater flow systems and the yellow line in the clipped map shows location in the study area where each square is 1x1 km, the pink area indicates the extent of Figure 20.

6. Conclusions

Vertical hydraulic conductivity values from the infiltration tests are much higher than the maximum average daily rain intensity for fifty years (0.19 m/day) in land use areas of forest, coffee plantation and grass field. Thus, most of the net precipitation will likely infiltrate to the unsaturated zone at a rainfall event and not generate much direct runoff, the differences in infiltration rate between the different land use areas are neglectable. With the permeable soil and steep slopes water is likely to both enter and leave the unsaturated zone quickly and possibly repeatedly. The extraction of water from all springs assessed has a big effect on the natural flowrates in the streams and rivers, and possibly also on spring flow rates in downstream areas. The amount and at which time water extraction occur are therefore more worrisome than the change in land use in a sustainable water resources perspective.

The data analysis of precipitation and spring flow indicates on a potential water age between 0-24 months in the aquifers communicating with ASADA-springs in the study area. The recent decrease of flow in the ASADA-springs can therefore be explained by the less than average precipitation in the last two years. The range of 24 months are explained by oblong recharge areas and that multiple groundwater flow systems discharge in the same spring.

From previous studies it was found that the water age of the layer Bermúdez is 10-15 years (Gomez, 1987). The groundwater communicating with the ASADA-springs are therefore most likely not originating from Bermúdez but more likely from the top lava layer Bambinos. The Colima formation with aquifer layers below the Barva formation is only found in one of the drilled wells close to the study area and a possible flow system in this formation could not be connected to the springs assessed. However, it is not precluded that regional groundwater flow could occur in the Colima Formation and become MBR from catchments in the high-altitude study area.

The four catchments linked to a specific ASADA-spring, in the water balance analysis, shows both positive and negative yearly ΔS . Some of the ASADA-springs could therefore be connected to more than one type of flow system which can explain the spring flow rate patterns being affected by precipitation in both short terms but also up to 2 years afterwards. No groundwater levels were measured, and therefore no conclusion about the storage over time and at what depth the groundwater flow systems circulate could be determined.

6.1 Recommendations

To estimate recharge areas more accurately and to improve ΔS calculations, the interaction between the unsaturated zone and aquifers needs be further investigated. Measurements of groundwater levels are recommended to better understand where this interaction occurs and are also relevant for quantifying storage and transport of water in different layers and depths.

Both infiltration tests and flow measurements in rivers needs to be conducted in the rainy season to predict the recharge pathways more accurately, since it is possible that conditions change over the year with distinct weather seasons. Flow measurements in rivers and springs on a regional level are also recommended to investigate long-term effects further down the volcano affected by the water management in the high-altitude catchments and how it finally effects MBR.

References

- Alvarado Induni, G.E. (2011). Los volcanes de Costa Rica: Geología, historia, riqueza natural y su gente. San José: Editorial Universidad Estatal a Distancia.
- Andisol. (2011). In *Encyclopædia Britannica*. Retrieved August 25, 2020, from <https://www.britannica.com/science/Andisol>
- Arias, M. (2014). Estudio Hidrogeológico en el sector norte del cantón central de Alajuela, Costa Rica.
- Arredondo, S. (2011). Perforación de pozos horizontales para mejorar el abastecimiento y mitigar los racionamientos de agua potable en Heredia, Costa Rica. San José: Universidad de Costa Rica.
- ASADA, Carrizal. (2020). Flow measurements of springs. Unpublished.
- Bowes, D. R. (1990). Volcanic breccia. In *Petrology* (pp. 599–601). Boston, MA: Springer US. doi:10.1007/0-387-30845-8_254
- Brassington, R. (2017). *Field Hydrogeology* (4 ed.). New Jersey: John Wiley & Sons Ltd.
- Fetter, C. (2014). *Applied Hydrogeology* (4th ed.). Essex: Pearson Education Limited.
- Fodor, N., Sandor, R., Orfanus, T., Lichner, L., & Rajkai, K. (2011). Evaluation method dependency of measured saturated hydraulic conductivity. *Geoderma*, 165(1), 60-68. doi:<https://doi.org/10.1016/j.geoderma.2011.07.004>
- Freeman, T. G. (1991). Calculating catchment area with divergent flow based on a regular grid. *Computers and Geosciences*, 17(3), 413-422.
- Gaba, E. (2008) Blank relief map of Costa Rica for geo-location purpose (Wikimedia Commons) Retrieved September 29 , 2020. https://commons.wikimedia.org/wiki/File:Costa_Rica_relief_location_map.jpg
- Gomez, L. (1987). Evaluación del potencial de los acuíferos y diseño de las captaciones de agua subterránea en la zona de Puente de Mulas, provincia de Heredia, Costa Rica. Heredia: Universidad de Costa Rica.
- Hargreaves, G. H., & Merkle, G. P. (1998). *Irrigation fundamentals*. Colorado: Water Resources Publications.
- Huang, J., Wu, P., & Zhao, X. (2012). Effects of rainfall intensity, underlying surface and slope gradient on soil infiltration under simulated rainfall events. *Catena*, 104, 93-102.
- ISRIC – World Soil Information (2020). SoilGrids. Retrieved May 20, 2020 from <https://soilgrids.org/>
- Johnson, A. (1963). A Field Method for Measurement of Infiltration. Geological Survey Water-Supply Paper 1544-F. Washington: US Geological Survey; US Department of the Interior. Retrieved from <https://pubs.usgs.gov/wsp/1544f/report.pdf>
- Losilla Penón, M. (2010). Mapa Hidrogeológico del cantón de Alajuela. Programa de Investigación y Desarrollo Urbano Sostenible, Universidad de Costa Rica.

- Markovich, K. H., Manning, A. H., Condon, L. E., & McIntosh, J. C. (2019). Mountain-Block Recharge: A Review of Current Understanding. *Water Resources Research*, 55(11), 8278-8304.
- Narasimhan, T. (2009). *Hydrological Cycle and Water Budget*. University of California at Berkeley, CA, USA.
- Nelson, S. A. (2017). *Volcanic Landforms, Volcanoes and Plate Tectonics*. Retrieved June 23, 2020, from https://www.tulane.edu/~sanelson/Natural_Disasters/volclandforms.htm
- ONU. (1972). *Manual de instrucciones, estudios hidrológicos*. San José: ONU Publ. No 70.
- Or, D., Tuller, M., & Wraith, J. M. (2018). *Vadose Zone Hydrology/Environmental Soil Physics*. Zurich: Or, Dani; Tuller, Markus; Wraith, Jon M.
- Protti, R. (1986). *Geología del flanco sur del volcán Barva, Heredia, Costa Rica*. Heredia: Boletín de Vulcanología.
- Ramírez, R. (2007). *Recarga Potencial del Acuífero Colima y Barva, Valle Central, Costa Rica*. SERVICIO NACIONAL DE AGUAS SUBTERRÁNEAS RIEGO Y AVENAMIENTO.
- Rosetta Commons. (2003). *Rosetta Lite v1.1*. Retrieved May, 2020.
- Scanlon, B. R., Healy, R. W., & Cook, P. G. (2002). Choosing appropriate techniques for quantifying groundwater recharge. *Hydrogeology Journal*, 10, 18-39.
- Schosinsky, G. (2005). *Estudio Hidrogeológico de las Nacientes Prudencio*.
- Schosinsky, G. (2006). Cálculo de la recarga potencial de acuíferos mediante un balance hídricos de suelo. *Revista Geológica de América Central*, 34-35, 13-30. Retrieved from <https://www.redalyc.org/articulo.oa?id=45437342002>
- Schosinsky, G. & Losilla, M. (2000). Modelo analítico para determinar la infiltración con base en la lluvia mensual. *Revista Geológica de América Central*, 23, 43-55.
- SENARA. (2020). *Precipitation data from Los Cartagos weather station*. Unpublished.
- Springer, A. & Stevens, L. (2009). Spheres of discharge of springs. *Hydrogeology Journal*. 17. 83-93. 10.1007/s10040-008-0341-y.
- Tóth, J. (1963). A theoretical analysis of groundwater flow in small drainage basins. *Journal of Geophysical Research*, 68(16), p4795–4812.
- Tuff. (2020). In *Encyclopædia Britannica*. Retrieved August 17, 2020, from <https://www.britannica.com/science/tuff>
- U.S. Geological Survey. (2016). *Igneous and metamorphic-rock aquifers*. Retrieved August 14, 2020, from <https://water.usgs.gov/ogw/aquiferbasics/volcan.html>

Appendix

A: Available data

Figure 22 shows the annual precipitation in the unit mm/year with year on the horizontal axis. Figure 23 shows percentages in lower or higher than the mean value for each year. The two graphs are made with data from SENARA (2020).

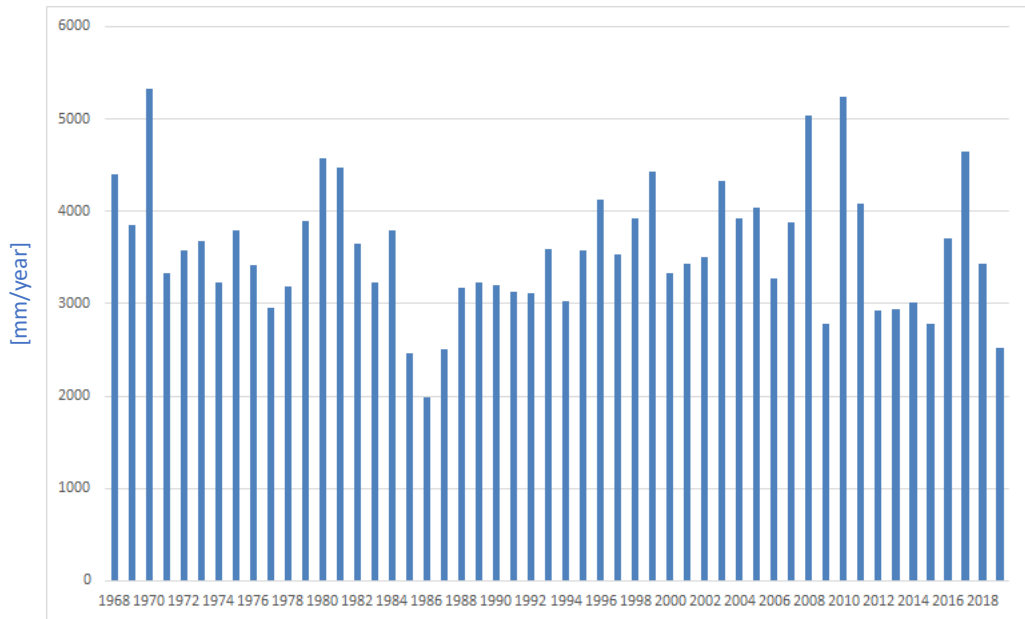


Figure 22 Annual precipitation at the weather station in Los Cartagos

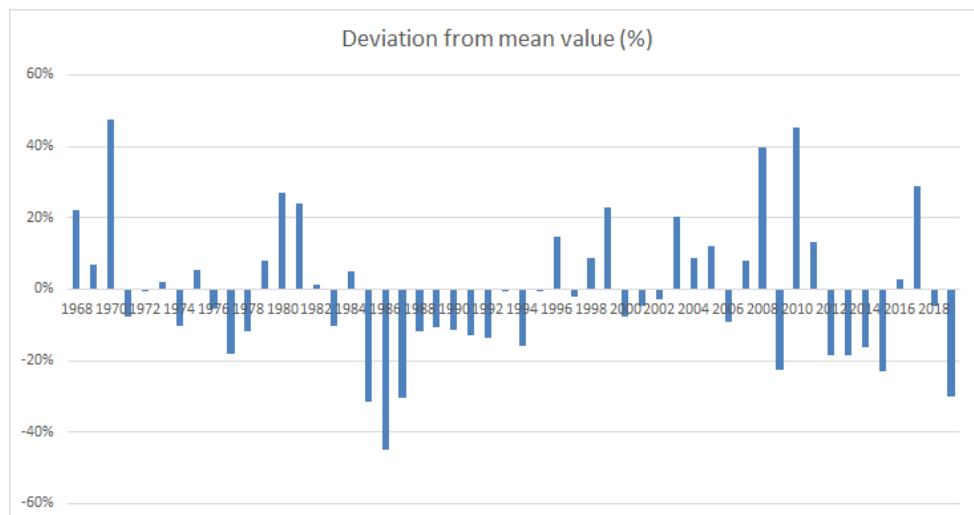


Figure 23 Annual percentage deviation from precipitation mean value, Los Cartagos weather station

Table 9. Monthly values of average flow in 4 springs (ASADA, 2020) and accumulated precipitation from Los Cartagos (SENARA, 2020)

Month	Precipitation (mm)	Virgen(l/s)	Prudencio (l/s)	Laguna (l/s)	Chomorro(l/s)
September	252.00	62			
October	219.00	42.42			
November	371.00	49.57			
December	463.00	59.31			
January (2010)	53.10	52.01			
February	406.50	45.14			
March	229.70	32.13			
April	243.10				
May	321.00	35.59			
June	282.60	23.01			
July	549.00	45.06			
August	358.00	51.22			
September	761.50	66.62			
October	894.10	92.73			
November	251.10	80.92			
December	532.80	67.46			
January (2011)	405.10	68.29			
February	192.20	61.81			
March	94.00				
April	16.42	45.11			
May	40.40				
June	233.90	38.88			
July	460.80	46.78			
August	345.10	41.79			
September	420.70				
October	263.80	57.37			
November	1006.10	76.1			
December	503.30	62.73			
January (2012)	507.70	60.03			
February	116.00	58.11			
March	70.10	47.55			
April	132.70	44			
May	101.10	40.52			
June	334.70	39.73			
July	406.10	40.49			
August	232.80	36.07			
September	279.60	41.29			
October	161.40	56.62			
November	237.60	47.47			
December	709.00	40.91			
January (2012)	152.30	37.75			
February	26.50	34.96			
March	108.90	29.04			
April	55.00	23.38			
May	364.30	22.19			

June	307.80	22.74			
July	281.60	21.06			
August	208.30	20.74			3.4
September	658.20	57.71			3.79
October	645.10	74.27			3.82
November	244.10	65.33			3.74
December	31.60	53.25			3.93
January (2014)	106.4	46.3		1.41	3.89
February	6.6	35.05		2.02	3.58
March	7.4	28.4		1.09	3.24
April	122.1	23.32		1.24	3.02
May	245.3	20.87		1.27	3.21
June	433.8	22.28		1.22	3.09
July	347.8	17.75		1.34	3.07
August	216.4	10.24		1.78	2.28
September	458.9	21.82		3.02	3.41
October	246.4	49.76		2.42	3.04
November	278.7	41.1		2.06	3.08
December	549.6	34.34		1.79	3.12
January (2015)	188.9	32.89		1.72	3.33
February	145.4	24.8		1.5	3
March	37.1	17.34		1.24	3.2
April	81.8	14.55		1.41	3.06
May	283.7	13.1		1.32	2.92
June	421.3	13.57		1.19	3.12
July	362.2	12.31		1.3	3.06
August	94.2	11.63		1.04	2.95
September	350.3	16.53		2.22	2.99
October	411.4	26.69		2.83	3.54
November	257	50.98		2.71	3.1
December	149.5	43.06		1.86	3.22
January (2016)	25.4	31.63	18.09	1.6	3.52
February	167.7	21.72	13.69	1.49	3.22
March	5.3	17.69	10.74	1.28	3.25
April	115	15.64	8.28	1.13	2.91
May	266.5	12.58	6.39	1.06	3.31
June	390.2	14.37	5	1.48	2.86
July	215.8	11.52	5.2	1.28	2.74
August	319.3	11.37	5.85	1.45	2.82
September	428.6	23.6	15.45	1.88	3.4
October	661.9	58.96	28.01	2.69	3.3
November	809.5	50.73	29	2.74	3.58
December	295.4	64.46	29.21	2.2	3.76
January (2017)	241.7	54.65	26.34	1.87	3.78
February	24.1	50.59	23.4	1.64	4.03
March	68.2	41.17	24	1.41	3.98
April	269	32.2	16.52	1.44	3.6
May	814	41.37	17.13	2.38	3.87
June	354.6	46.05	23.44	2.49	3.59
July	300	46.5	23.53	2.82	3.8
August	353.4	52	25.64	1.63	3.7
September	684.8	64.6	33.27	4.95	4.29

October	661.6	82.45	40.66	3.83	3.87
November	296.4	77.97	38.84	2.82	4.28
December	575.6	64.56	35.35	1.93	4.09
January (2018)	705.2	57.92	32.98	1.91	4.19
February	51.2	62.39	29.95	1.84	4.09
March	8.8	53.23	26.91	1.56	4.2
April	94.4	44.57	21.21	1.49	3.95
May	456.4	41.05	17.44	2.11	3.93
June	394.5	40.53	16.9	1.77	3.67
July	562.4	41.55	18.75	2	3.79
August	313.7	44.21	19.65	1.83	3.43
September	307.6	48.9	25.78	2.64	3.78
October	251.8	50.13	35.21	2.18	3.95
November	175.4	44.04	26.19	1.86	3.56
December	115.4	25.11	24.46	1.69	4.22
January (2019)	16.2	29.42	20.72	1.5	3.92
February	20.8	22.11	15.51	1.39	3.81
March	26.4	19.83	11.61	1.3	3.79
April	72.8	20.47	8.44	1.26	3.46
May	411.8	1.08	6.17	1.26	3.18
June	236.4	16.4	4.94	1.2	2.85
July	266.9	8.59	3.98	1.11	2.97
August	250.2	5.78	2.65	1.14	2.92
September	219.8	11.8	2.79	0.39	2.65
October	554.8	21.86	10.56	2.34	3.49
November	267	16.94	12.2	1.63	3
December	183.6	15.81	10.72	1.44	2.77
January (2018)		19.24	7.29	1.31	3.13
February		18.87	6.13	1.05	3.05

Table 9. The parameters for the Blaney and Criddle equation and corresponding monthly evapotranspiration. The temperature and percent sunlight are average values for the years 1999-2012 and originates from the weather station Estacion Fraijanes (30 kilometres from Carrizal).

	Average temperature [°C]	Average percent of daily sunlight	Days without rain per month	Days per month	Actual Evapotranspiration [mm/month]
Jan	16.2	8.13	26	31	20
Feb	16.6	7.47	19	29	41
Mar	17	8.45	28	31	13
Apr	17.7	8.37	21	30	41
May	17.8	8.81	9	31	102
Jun	17.7	8.6	4	30	121
Jul	17.6	8.86	7	31	111
Aug	17.6	8.71	7	31	109
Sep	17.4	8.25	4	30	115
Oct	17.1	8.34	2	31	125
Nov	17	7.91	3	30	113
Dec	16.7	8.1	6	31	103

B: Springs

Table 10. Individual characteristic information of springs, X/Y coordinates in CRTM05

Spring name	Vertical distance from nearby major stream (m)	Slope at spring Gentle (<45°) Steep (>45°)	Flow Low (< 4) l/s) High (>4 l/s)	Visible block and stones	X	Y
Prudencio	0-5	Gentle	High	Yes	483701,53	483701,53
Virgen	5+	Steep	High	Yes	482920,82	1116567,05
Virgen 2 (small)	0-5	Gentle	Low	Yes	- -	- -
Chomorro	5+	Steep	Low	Yes	482775,95	1116344,81
Laguna	0-5	Gentle	Low	No	482148,95	1115219,45
Ahogados	0-5	Gentle	Low	Yes	S-W of Laguna	-
Diogenes	0-5	Gentle	-	Yes	483489,44	1116821,81
Zaguates TOP	5+	Steep	Low	Yes	484810,65	1117443,45
Lomas	5+	Steep	High	Yes	483769,76	1117505,95
Victor 1	5+	Steep	Low	No	483514,36	1117890,50
Victor 2	0-5	Gentle	Low	Yes	483793,24	1118291,51
Victor 3	0-5	Gentle	-	Yes	483953,54	1118715,69
Victor 4	5+	Gentle	Low	Yes	483941,07	1118509,44
Ana 1	0-5	Gentle	Low	Yes		
Ana 2	0-5	Gentle	Low	Yes		
Ana 3	0-5	Steep	Low	Yes		
Upstream Ahogados	5+	Steep	-	Yes	483701,53	1116160,99

C: Data analyses

Result plots from scenarios made by the Annual comparison in Section 5.2.

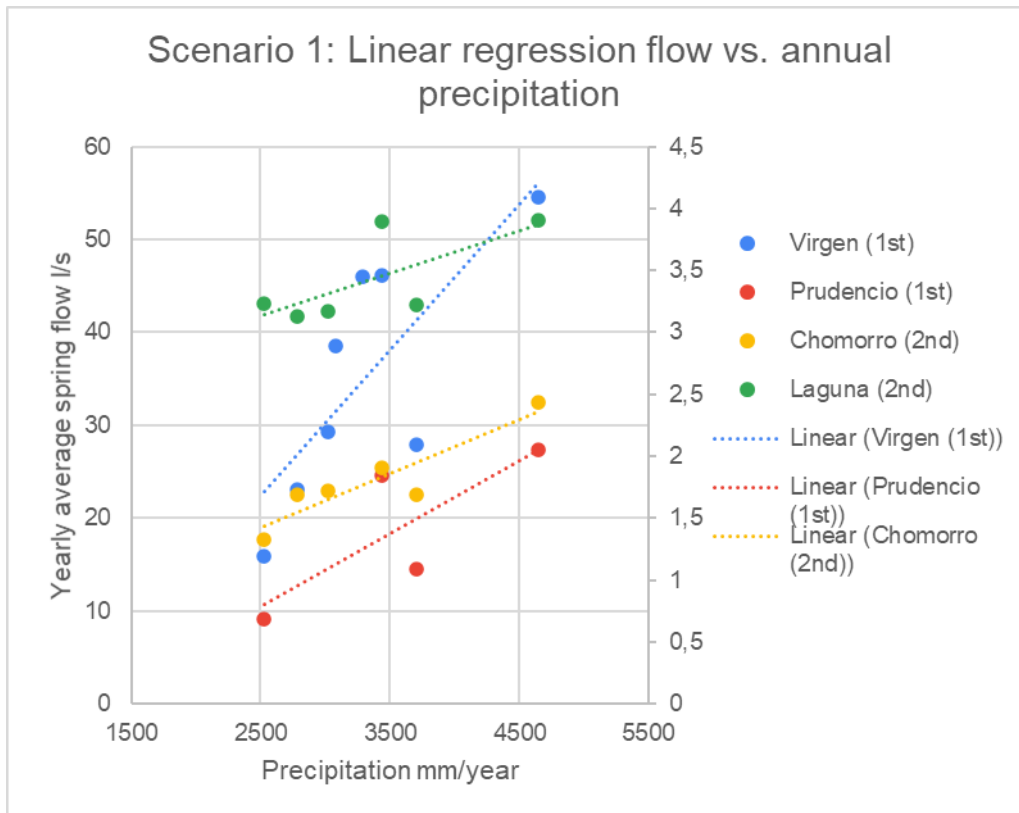


Figure 24. Linear regression of average yearly spring flow versus total precipitation of one year, scenario 1..

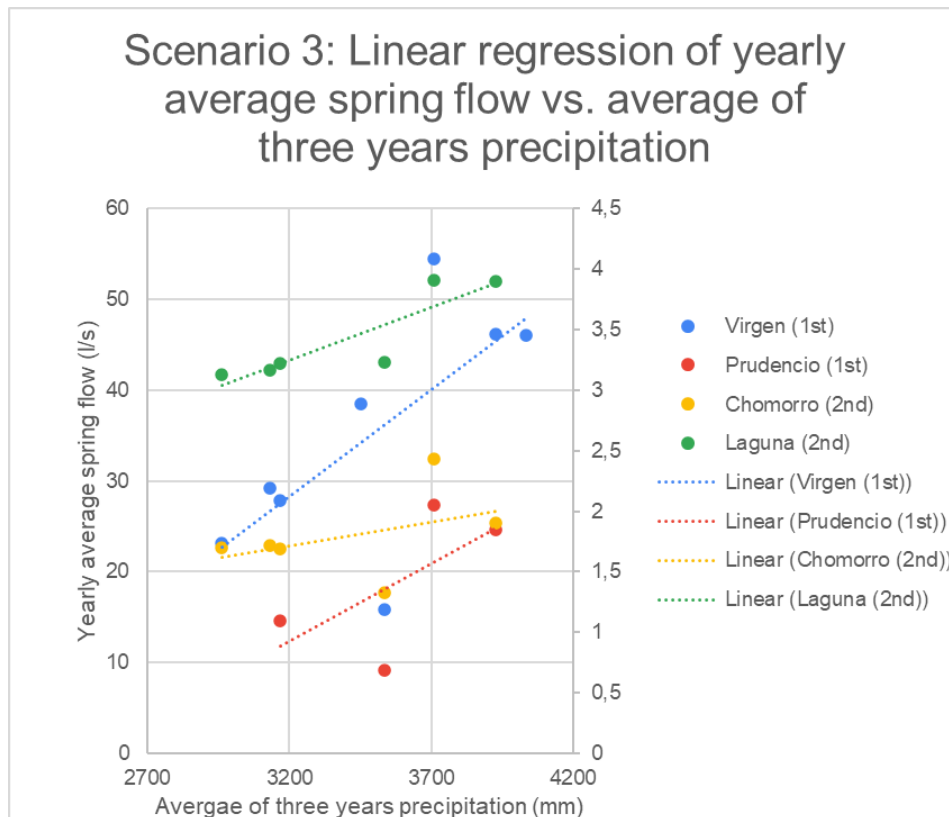


Figure 25. Linear regression of average yearly spring flow versus average total precipitation of three years, scenario 3.

Table 11 Parameters for calculations of infiltration method I2.

Spring	Land use	F [mm/day]	K_{FC}	K_P	Slope	K_V	C
Virgen	Grassland	1230	0.9872234427	0.06	0.07	0.18	1
Prudencio	Coffee	1490	0.9983838835	0.06	0.07	0.1	1
Laguna	Coffee	1490	0.9983838835	0.06	0.07	0.1	1
Chomorro	Forest	8330	1	0.06	0.07	0.2	1

D: Well Reports

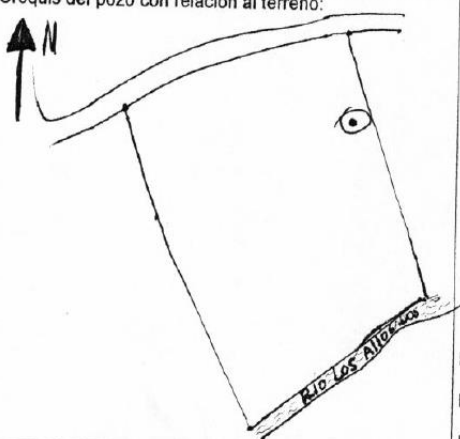
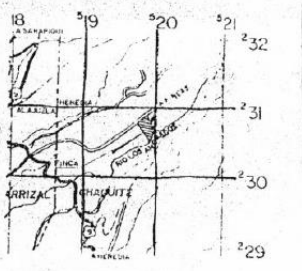

REPORTE FINAL DE PERFORACIÓN Página 1		Empresa perforadora: PERFORACIONES JIMENEZ Y DELGADO, LTDA	
Pozo Número: BA-727	Bitácora No. 1242-01 CGCR	UBICACIÓN CARTOGRÁFICA (Dibuje el cuadrante)	
Localidad: Santa Barbara de Heredia			
Croquis del pozo con relación al terreno: 		LOCALIZACIÓN 	
Propietario: HUGO A. JIMENEZ BASTOS		Hoja: BARVA	No. 3346-II
		Escala: 1: 50.000	Latitud: 230.800
		Longitud: 519.950	
Uso que se dará al agua: Doméstico	Método de perforación: Percusión	Equipo de perforación: 22 W-3	
Inicio de perforación: 23-11-2001	Final de perforación: 7-12-2001	Profundidad total: 80 metros	
VARIACIÓN DE NIVEL DE AGUA Y AVANCE DE LA PERFORACIÓN		DESCRIPCIÓN LITOLÓGICA DETALLADA	
Prof. (m)	Nivel (m)	Tramo (m)	Descripción
39.00	35.00	0,00-13,00	Suelo vegetal. Permeabilidad aparente baja.
		13,00-28,00	Arcillas color café. Permeabilidad aparente baja
		28,00-39,00	Cantos rodados. Permeabilidad aparente regular.
		39,00-50,00	Lavas color gris. Permeabilidad. Permeabilidad aparente regular.
		50,00-62,00	Rocas escoriáceas color rojizo. Permeabilidad aparente buena.
		62,00-80,00	Brechas color rojizo. Permeabilidad aparente muy buena.
			
CONDICIONES HIDROGEOLÓGICAS ENCONTRADAS			
El acuífero se genera en las rocas escoriáceas y brechas rojizas, en donde la permeabilidad es bastante buena. Los caudales de extracción en esta formación es del orden de los 3.00 y hasta 10 litros por segundo.			

Figure 26. Drill report of well BA-727

REPORTE DE PERFORACION página 1		EMPRESA PERFORADORA HIDROMAQ S.A.															
Pozo número BA-786		Bitacora N° 1616-02 CGCR															
Localidad: Carrizal de Alajuela																	
		UBICACIÓN CARTOGRAFICA Hoja: Barva No. 3346-II Escala 1:50.000 a.s.n.m.: 1450m. Latitud: 229.550 Longitud 517.400															
Propietaria: Everdast de Costa Rica																	
Uso que se dará al agua: Riego de Invernadero		Método de perforación Percusión a cable	Equipo de perforación: Bucyrus Erie 22W Serie 2														
Inicio de perforación: 10 de junio del 2003		Final de la perforación: 24 de junio del 2003	Profundidad Total: 82m.														
VARIACION DE NIVEL DE AGUA Y AVANCE DE LA PERFORACION:		DESCRIPCION LITOLOGICA DETALLADA:															
<table border="1"> <thead> <tr> <th>Prof. (m)</th> <th>Nivel (m)</th> </tr> </thead> <tbody> <tr> <td>0 - 26</td> <td>0</td> </tr> <tr> <td>26 - 30</td> <td>24.0</td> </tr> <tr> <td>24 - 60</td> <td>24.0</td> </tr> <tr> <td>60 - 66</td> <td>54.0</td> </tr> <tr> <td>66 - 72</td> <td>65.0</td> </tr> <tr> <td>72 - 82</td> <td>69.42</td> </tr> </tbody> </table>	Prof. (m)	Nivel (m)	0 - 26	0	26 - 30	24.0	24 - 60	24.0	60 - 66	54.0	66 - 72	65.0	72 - 82	69.42	0-4m. Cenizas volcánicas arcillificadas, de color café amarillento. 4-8m. Piroclastos arenosos, sueltos, fragmentos alterados, color café, clastos de pómez, escoria volcánica, angulosas. Permeabilidad aparente buena. Arenón Poasito. 8-16m. Arcillas de color café, impermeable, livianas. 16-20m. Paleosuelo arcilloso rojizo, impermeable. 20-26m. Arcilla de color café, suave, ligeras, impermeables. 26-36m. Lahar arcilloso con clastos muy alterados, color amarillento. 36-60m. Lava volcánica de color gris claro, alterada, muy fracturada. Permeabilidad aparente buena. 66-70m. Ignimbrita de color grisáceo, suelta, freable, clastos de lava, pómez. Permeabilidad aparente moderada. 70-78m. Ignimbrita de color gris claro con clastos de lava, escoria, pómez, suave. Permeabilidad aparente buena. 78-82m. Lava volcánica andesítica, de color gris oscuro, muy fracturada. Permeabilidad aparente muy buena. Acuífero.		
Prof. (m)	Nivel (m)																
0 - 26	0																
26 - 30	24.0																
24 - 60	24.0																
60 - 66	54.0																
66 - 72	65.0																
72 - 82	69.42																

Figure 27. Drill report of well BA-786